

4592

Hematological Response Elicited by Nanobead Based Targeted Drug Delivery in Leukemic Rat Model



By
Anum Tahir

Department of Biochemistry
Faculty of Biological Sciences
Quaid-i-Azam University
Islamabad, Pakistan

2016



Hematological Response Elicited by Nanobead Based Targeted Drug Delivery in Leukemic Rat Model

A thesis submitted in partial fulfillment of the requirements for the
Degree of

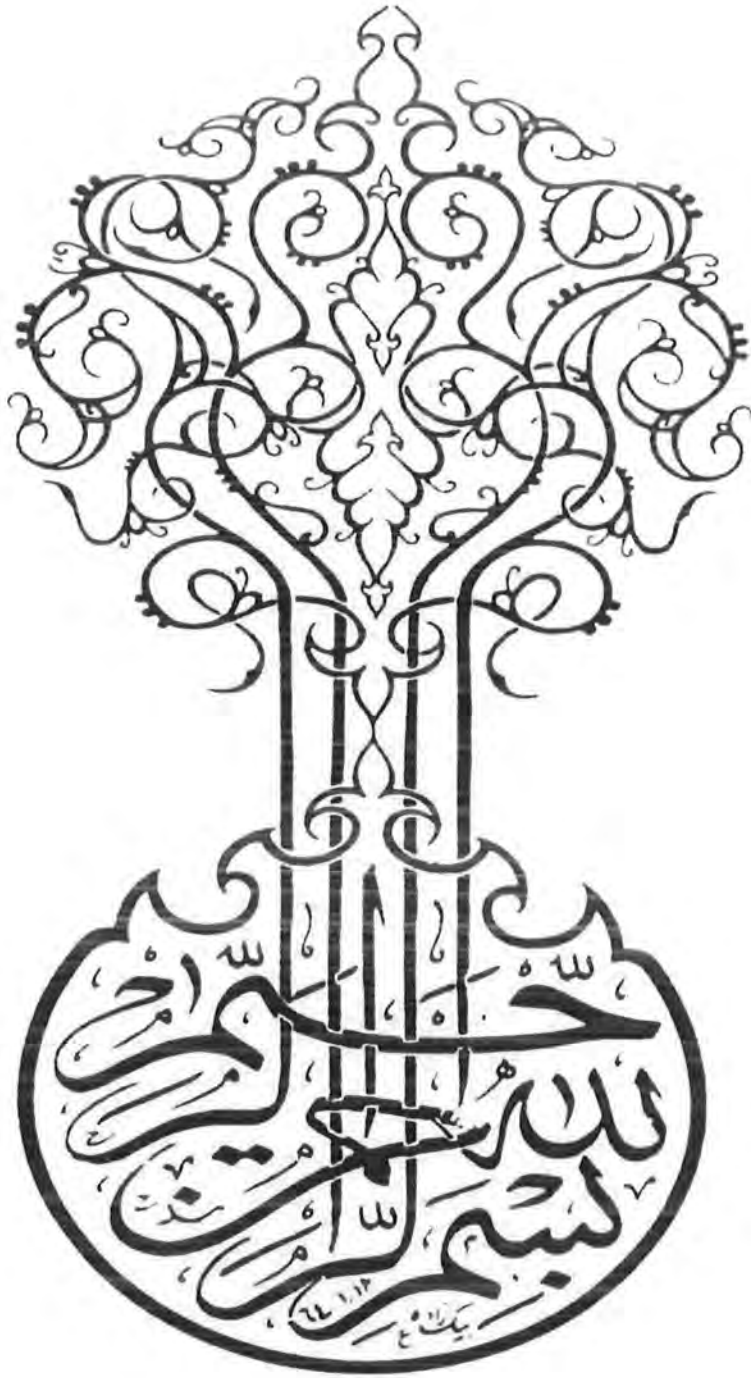
Master of Philosophy in Biochemistry



By
Anum Tahir

Department of Biochemistry
Faculty of Biological Sciences
Quaid-i-Azam University
Islamabad, Pakistan
2016





In the name of ALLAH, Most Gracious, Most Merciful.

"Read! In the Name of your Lord who has created (all that exists). He has created man from a clot. Read! And your Lord is the Most Generous. Who has taught the writing by the pen. He has taught the man that which he knew not"

[Quran, 96: 1-5]

Declaration

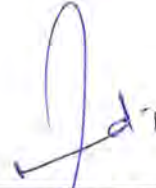
The material and information contained in this thesis is my original work. I have not previously presented any part of this work elsewhere for any other degree.

Anum Tahir

CERTIFICATE

This thesis, submitted by **Ms. Anum Tahir** to the Department of Biochemistry, Faculty of Biological Sciences, Quaid-i-Azam University, Islamabad, Pakistan, is accepted in its present form as satisfying the thesis requirement for the Degree of Master of Philosophy in Biochemistry/Molecular Biology.

Supervisor:



Dr. Shahid Waseem
Assistant Professor

External Examiner:



Dr. Kehkashan Mazhar
Principal Scientific Officer
Dr. A.Q. Khan Research Laboratories
G-9/1, Islamabad..

Chairman:



Dr. Muhammad Ansar
Associate Professor

Dated:

March 21, 2016

List of Contents

S. No.	Title	Page No.
1.	Acknowledgments	i
2.	List of Abbreviations	iii
3.	List of Figures	v
4.	List of Tables	vii
5.	Abstract	viii
6.	Introduction	01
7.	Materials and Methods	19
8.	Results	26
9.	Discussion	41
10.	References	45

Acknowledgements

All praises to Almighty Allah, the Omnipotent, the most Compassionate and His Prophet Muhammad (P.B.U.H.), who is a source of guidance and knowledge for humanity as a whole.

I feel highly privileged in taking opportunity to express my profound gratitude to my worthy supervisor **Dr. Shahid Waseem**, Assistant Professor, Quaid-i-Azam University, Islamabad for his skillful guidance, affectionate criticism, positive attitude, motivational support and keen interest in my work. It was because of him, I gained exposure in finest research facilities namely National Centre for physics (NCP), Islamabad.

I further extend my utmost gratitude to **Dr. Samina Nazir** (co-supervisor at NCP), as without her support and guidance I wouldn't be able to achieve my goal.

I am thankful to **Dr. Muhammad Ansar**, Chairperson, Department of Biochemistry, Quaid-i-Azam University, Islamabad, Pakistan for providing me all possible facilities.

I am highly obliged to all faculty members from Department of Biochemistry, Quaid-i-Azam University, Islamabad, for their constructive and necessary guidance and scholastic criticism during the entire tenure of degree and dissertation write up.

I am indebted to my younger brother **Anab Tahir** for his appreciation and moral support and motivation at each step. I extend my profound gratitude to my fiancé **Mr. Adnan Abbasi** who cherished heartiest wishes for me. I can never forget prayers, untiring efforts and encouragement of my mother in law, brother **Mr. Imran Abbasi**, my sisters **Sadia Abbasi, Nadia Mussayab, Shaista Abbasi and Faiza Hayat**.

I wish to extend my gratitude to, my very dearest friend **Sidra Bukhari** for her presence in every trouble and beautiful time we spent together. I am thankful to worthy fellows **Sohail Baloch, Irum Shehzadi, Zain Ali, Rabia Ghaffoor, Huzaifa Hanif** and my humble senior **Tauseef Rehan** for their continuous motivation, support and positive input for all the decisions of my life in addition to my studies.

I owe big thanks to my friends **Mohsina Batool, Urooj Nazir, Sadia Zafar, Rahat Riaz, Iqra Aslam, Nosheen Masood, Sahar Mahrin and Anum Saleem** for their support, encouragement, concern, shared laughter and for taking their time to listen to everything that I had to say.

At the end I would like to thanks **Mr. Amir, Mr. Fiaz, Mr. Tariq** and **Mr. Shehzad** for their good behavior and support at every step during my studies.

Anum Tahir



List of Abbreviations

ALL	Acute lymphocytic leukemia
AML	Acute myeloid leukemia
ATO	Arsenic trioxide
ATRA	All-trans-retinoic acid
Ba	<i>Ocimum basilicum</i>
CLL	Chronic lymphoblastic leukemia
cm ⁻¹	Centimeter
CMC	Carboxymethyl cellulose
CML	Chronic myeloid leukemia
CNH	Carbon nano horns
CNTs	Carbon nanotubes
CTAB	Cetyltrimethylammonium bromide
DDS	Drug delivery system
DLS	Dynamic light scattering
DMSO	Dimethyl sulfoxide
DNA	Deoxyribonucleic acid
EC	Ethyl cellulose
EDTA	Ethylene diamine tetraacetic acid
ERK5	Extracellular signal-regulated kinase 5
FTIR	Fourier Transform Infrared Spectrophotometer
FWHM	Full Width at Half Maximum
H ₂ O ₂	Hydrogen peroxide

HL-60	Human Promyelocytic leukemia cells
HO[•]	Hydroxyl radicals
IPA	Isopropanol
KBr	Potassium bromide
mRNA	Messenger Ribonucleic acid
MSNPs	Mesoporous silica nanoparticles
MWCNTs	Multi walled carbon nanotubes
NaOH	Sodium Hydroxide
NARC	National Agriculture Research Center
NIH	National Institute of Health
NK	Natural killer
Nm	Nanometer
O	Oxygen
PBS	Phosphate Buffer Saline
RM	Rosmarinus officinalis
SEM	Scanning electron microscopy
SWNCTs-	Single Walled Carbon Nanotubes
TEM	Transmission Electron microscopy
TEOS	Tetraethyl orthosilicate
TH	<i>Thymus vulgaris</i>
UV-VIS	Ultraviolet visible
WBCs	White blood cells
XRD	X-ray diffraction spectroscopy
µm	micro meter

List of Figures

Title	Page No.
Fig 1 Schematic representation of leukemia induction and treatment with extract-loaded MSNPs in 5 groups of rats	24
Fig 2 XRD Pattern of MSNPs	27
Fig 3 SEM of MSNPs	27
Fig 4 Absorbance spectra of MSNPs, crude extracts and extract loaded MSNPs. (a), MSNPs; (b) RM crude extract; (c), RM-loaded MSNPs; (d) TH crude extract; (e), TH-loaded MSNPs; (f), Ba crude extract; (g), Ba-loaded MSNPs	28,29
Fig 5 FTIR of RM-loaded MSNPs with soluble starch coating. (a) MSNPs; (b) RM crude extract; (c) RM coated MSNPs; (d) soluble starch; (e) final loading product MSNPs, RM and soluble starch	30
Fig 6 FTIR of TH-loaded MSNPs with EC coatings. (a) MSNPs; (b) TH crude extract; (c) TH-loaded MSNPs; (d) EC; (e) final loading product MSNPs, TH and EC	31,32
Fig 7 FTIR of Ba-loaded MSNPs with CMC coatings. (a) MSNPs; (b) Ba crude extract; (c) Ba-loaded MSNPs; (d) CMC ; (e) final loading product MSNPs, basil and CMC	33
Fig 8 Comparison of relative organs weight of control, leukemic and treated groups of rats.	34
Fig 9 Differential count of WBCs in rats induced with benzene. Control; (W1) week 1 and (W2) after benzene administration	35
Fig 10 Differential count of WBCs in rats after benzene administration and treatment with MSNPs loaded plant extracts. W2, (week 2 of benzene); RM, (Rosmarinus officinalis loaded MSNPs); TH, (thymus vulgaris loaded	36

	MSNPs) and Ba (<i>Ocimum basilicum</i> loaded MSNPs).	
Fig 11	Bone Marrow of normal, leukemic and treated rats. (a), control BM; (b) benzene treated; (c), RM-loaded MSNPs; (d), TH-loaded MSNPs; (e), Ba-loaded MSNPs treated. Where MB indicates myeloblasts; P, pro-myelocyte; M, late myelocyte; NSN, non-segmented neutrophil (band); SN, segmented neutrophil; Er, erythroid precursor.	38
Fig 12	Erythrophagocytosis shown by leukemic rat.	39
Fig 13	Blood cells morphology. (a) , Normal; (b), benzene treated; (c) RM-loaded MSNPs; (d), TH-loaded MSNPs ; (e), Ba-loaded MSNPs treated rats	40

List of Tables

S. No.	Title	Page No.
Tab 1.	Chemicals used in MSNPs synthesis and coating	19
Tab 2.	Reagents used in leukemia induction and blood cells staining	24
Tab 3.	Calculation of MSNPs diameter from Scherrer equation	26

Abstract

Nanoparticle mediated chemotherapy against leukemia would be more effective as compared to the native drug. The present study aimed to synthesize drug-loaded mesoporous silica nanoparticles (MSNPs) to investigate hematological response in leukemic rat. SEM, XRD, FTIR and UV/VIS spectrophotometric data showed characteristic properties of generic MSNPs. Nano-scaled size (47.94 nm) MSNPs suitable drug carriers. Neutrophilia, lymphopenia and decreased monocyte level were observed after benzene induction. RM-, TH- and Ba-loaded MSNPs exhibited a capacity to minimize the impact of benzene (AML condition) as seen by differential count of WBC, relative organ weight analysis, morphological analysis and BM analysis. However, Ba-loaded MSNPs exhibited significant impact to improve cellular indicators as compared to RM- and TH-loaded MSNPs.

Introduction

1.1 Nanoparticles

Nanoparticles by definition are solid particles with a size in range of 10_1000nm. Drug is encapsulated, dissolved, entrapped or attached to nanoparticle surface (Mohanraj & Chen, 2007).

1.2 Nanoparticles Types

Different materials have been used to develop nanoparticles for therapeutic purposes.

1.2.1 Inorganic Nanoparticles

Inorganic composites i.e. alumina or silica typically compose ceramic nanoparticles. Inorganic nanoparticles may be porous and provide large surface area and entrapment of drug, protecting drug from degradation and denaturation. Hollow core silica particles are prepared that contain a central reservoir. Mesoporous silica nanoparticles particles are also formulated that contain “worm-like” network of channels throughout the central texture. Surface of these particles can be easily modified by single functionalities via variety of chemical alterations (Faraji & Wipf, 2009).

1.2.2 Polymeric Nanoparticles

Biodegradable polymeric nanoparticles have engrossed more attention in recent years as prospective drug delivery device because of their application in controlled drug release, their capability to target specific tissue, to carry peptides, proteins and genes and as a carrier of DNA in gene therapy (Soppimath *et al.*, 2001). Drug-biodegradable polymeric nano-carrier conjugates used as a drug delivery device are stable in blood, non-toxic, non-immunogenic, non-pro inflammatory and non-thrombogenic (Wilczewska *et al.*, 2012).

1.2.3 Carbon Nanomaterials

Carbon is also used as nanomaterials in the form of carbon nanotubes (CNTs) and Nano horns (CNH). CNTs are characterized on the basis of architecture formed by rolling of single (SWNCTs- single walled carbon nanotubes) or multi (MWCNTs – multi walled carbon nanotubes) layers of graphite with thermal conductivity and large surface area. In vivo studies concerning administration of nanotubes in rats induced changes in lung morphology i.e. granuloma formation and interstitial fibrosis (Muller *et al.*, 2005).

1.2.4 Magnetic Nanoparticles

Magnetic nanoparticles tend to be highly promising carriers of drug due to its wide variety of attributes. They can be handled easily by applying external magnetic field. Active and passive drug delivery strategies can be used to deliver magnetic nanoparticles. These nanoparticles can also be used in diagnostics through MRI. They are also actively up taken by tissues resulting in efficient drug delivery and effective treatment at optimal doses (Arruebo *et al.*, 2007). In most cases, these objectives are not achieved because of inappropriate magnetic system or lack of understanding regarding features of magnetic nanoparticles. Magnetic nanoparticles form aggregates losing the specificity connected to their Nano sized dimensions (Neuberger *et al.*, 2005).

1.2.5 Silica Nanoparticles

Silica particles provided an alternative to organic delivery systems due to their biocompatibility and hydrophobicity. They provide excellent protection to internal payload that make them perfect candidate for controlled drug delivery application (insert citation silica particles: a novel drug delivery system)

Silica has attracted great attention because it is cheap, thermally stable, harmless and chemically inert (Nandiyanto *et al.*, 2009).

Amorphous fumed silica has been proved safer as it showed minimum or no toxicity in previous studies (Barnes *et al.*, 2008) Potential applications of amorphous silica have encompassed areas in Nano biotechnology such as drug delivery, gene transfer, bioanalysis and imaging and diagnostics. It is probable that silica nanoparticles may be directed through all possible routes i.e. intravenous injection, orally, inhalation and transdermal delivery (Chang *et al.*, 2007)

1.3 Surface Characteristics and Nanoparticles Size

Nanoparticles used in drug delivery system must have capability to stay in blood stream for longer duration of time to efficiently deliver drug to targeted tumor tissue without being discharged from the body. Nanoparticles that are not modified are mostly trapped by liver and spleen dependent on their size and surface characteristics (Moghimi *et al.*, 2001).

1.3.1 Size

The greatest advantage of nanoparticles is that their size can be managed. Two things must be considered during size management.

1) They should be large enough to prevent their outflow into blood capillaries however, small enough to escape macrophage engulfment. The size of fenestra of the kuffer cells in liver and sinusoid in spleen varies from 150 to 200 nm (Wisse *et al.*, 1996).

2) Endothelial cells of dripping tumor vasculature have gap junction and its size may fluctuate from 100 to 600 nm. The size of nanoparticles should be up to 100 nm to reach target tissues by passing through these two specific vasculatures (Cho *et al.*, 2008).

1.3.2 Surface Characteristics

The one important factor, other than size of nanoparticles, is their surface characterization that determines the life span and fate in blood circulation relating to their capture by macrophages. Ideally, nanoparticles should have hydrophobic surface to escape from macrophage capture (Moghimi & Szebeni, 2003).

1.3.3 Characterization of Nanoparticles

Various techniques are used to study size, structure, absorption, porosity and various other properties of nanoparticles. These include:

- X-ray diffraction analysis (XRD)
- UV visible spectroscopy
- Scanning electron microscopy (SEM)
- Fourier transform infra-red spectroscopy (FTIR)
- Transmission electron microscopy (TEM)
- Dynamic light scattering (DLS)
- Atomic force microscopy
- Zeta potential

1.3.3.1 Scanning Electron Microscopy (SEM)

SEM is used to study surface structures, it is relatively simple experiment and minimum sample is required. It is used to obtain solid information on surface structures from non-projected images in three dimensions because the objective lens have long focal depth (Che *et al.*, 2003). Scanning electron microscopy (SEM), in which a tightly focused beam of electrons is raster-scanned over the specimen while secondary or backscattered electrons are detected, is used in biological imaging mostly as a surface visualization tool (Denk &

Horstmann, 2004). Process involves passing of x-ray beam through sample and inter particle spacing is measured.

1.3.3.2 X-ray Diffraction (XRD)

XRD depicts the characteristic peak of nanoparticles. Particle size can also be measured with the help of Debye-Scherrer formula, in X-ray diffraction and crystallography, it relates size of compound with the widening of peak in a refraction pattern.

$$D=0.9\lambda / \beta\cos\theta \dots\dots\dots (1)$$

$$2d\sin\theta=n\lambda \dots\dots\dots (2)$$

Where ‘ λ ’ shows wave length of X-Ray, ‘ β ’ is FWHM (full width at half maximum), ‘ θ ’ is the diffraction angle and ‘D’ is particle diameter size (John & Florence, 2009).

1.3.3.3 Fourier Transform Infrared Spectroscopy (FTIR)

FTIR is a technique used to get information about functional groups present in any substance. Spectra is recorded in mid infrared region (400_4000 cm^{-1}) on a spectrophotometer. FTIR studies also reveals the new chemical entities formation and also shows absorption bands of particular functional group that highlight characteristic of protein spectra in case of drug loading (Sarmiento *et al.*, 2006).

1.4 Nano Biotechnology

Nano biotechnology is an emerging field where Nano sized materials (5-500 nm) are used in various biological applications (Mohanraj & Chen, 2007). Nano sized materials are usually in the range of proteins and biological macromolecules (Faraji & Wipf, 2009). Nanoparticles retain unique physical properties which determine their role in biomedical sciences. As the size of particles is scaled down, physical and chemical properties show significant improvement. Nanoparticles of different materials are developed and

characterized for their role in biomedical sciences (Moghimi *et al.*, 2005). The most commonly used nanoparticles in drug delivery are silicon, iron, nickel, cobalt and silver. Various formulations of these nanoparticles have been considered for therapeutic application (Huang *et al.*, 2007; Sanvicens & Marco, 2008).

Drug coated nanoparticles can be used as therapeutic agents to treat various pathological conditions like cancer, allergies and inflammation etc. Encapsulated drug coated nanoparticles would be the choice which help in a sustained drug release over a period of time. It provides an intracellular sanctuary to protect therapeutic compounds from efflux or degradation (Faraji & Wipf, 2009).

Many different systems and approaches have been assessed for drug targeting to tumors over the years, including the following

1.4.1 Passive Targeting

Transport of Nano carriers through leaky vessels of endothelial tissues surrounding tumor microenvironment along with the fluids is called passive diffusion. Due to passive targeting there are more chances of drugs to reach tumor cells rather than normal ones (Haley & Frenkel, 2008).

1.4.2 Active Targeting

Surface of nanocarrier are attached with specific ligands for binding specific receptors expressed at target site, this type of targeting is called active targeting. Receptor overexpressed in tumor cells is chosen to deliver drug only to tumor tissues (Danhier *et al.*, 2010).

1.4.3 Stimuli-Responsive Drug Delivery

A new technique of targeting consists in development of activable nanocarrier. During circulation they carry stealth function, when it arrive at tumor site the tumor microenvironment allows drug release from nanocarrier. Drug release may be achieved upon interaction to some external stimuli, such as light, heat, magnetic fields (Lammers *et al.*, 2012).

1.5 Targeted Drug Delivery

To deliver a chemo-therapeutic compound selectively at a pathological site is an eminent problem in the cure of many diseases. A traditional application of drugs is characterized by inadequate bio-distribution, lack of selectivity and limited effectiveness (Wilczewska *et al.*, 2012). Controlled drug delivery system (DDS) can overcome these drawbacks and limitations. Controlled DDS can be designed to enhance the properties of conventional (free) drugs, their proper distribution and release at the target site (Allen & Cullis, 2004).

In controlled drug delivery systems (DDS) the pharmacologically active compound is transported selectively to the target site thus, its influence on healthy tissues and undesirable harm can be minimized (Wilczewska *et al.*, 2012).

The important points in formulating appropriate and effective controlled DDS are:

- a. Drug absorption and release
- b. Biocompatibility
- c. Functionality
- d. Stability and shelf-life
- e. Targeting and bio-distribution

1.5.1 Therapeutic Index

Drug coated nanoparticles used as therapeutic agents enhance drug delivery as well as uptake by target cells. It helps in reducing effect on non-targeted organs. It contributes to increase therapeutic index [the comparison of therapeutic effectiveness (tumor cell death) to the amount that cause toxicity to other organ systems] (De Jong & Borm, 2008).

1.5.2 Targeted Delivery of Nanoparticles

Ideally, therapeutic drugs should reach at pathogenic site, through penetration of body or cell barriers with minimum loss or action in blood circulation. Secondly, after drug has reached at its targeted site, it should have the ability to treat selectively the target tissues without harming normal cells with controlled release mechanism. These strategies are important in survival of patient with quality of life due to intracellular connection of drug and reducing dose-limiting toxicities. Nanoparticles seem to satisfy both requirements for effective drug delivery system (Cho *et al.*, 2008).

1.6 White Blood Cells

Body's immune response is mediated by diverse group of cells types that are called leukocytes or WBCs. Circulation of these cells is through blood and lymphatic system and they recruit the infectious site or damaged tissue. They originate from hematopoietic stem cells and develop according to distinct differentiated pathways depending upon internal and external cues (Porcher *et al.*, 1996). Cells of the immune system are as follows;

1.6.1 Neutrophils

Neutrophil components of innate immune system are the first immune cells that arrive at the infection site serving as first line of defense in body against pathogens. They release cytokines to innate inflammatory response and for induction of immune cells trafficking

they release chemokines. This allows adaptive immune system enough time for planning sterilizing immunity and memory. Neutrophils recognize pathogens by specific receptors present on them called Toll-like receptors (Hayashi *et al.*, 2003).

1.6.2 Monocytes

They circulate in blood, bone marrow and spleen. They also serve as first line of defense along with neutrophils. They have chemokine receptors and receptors for recognition of pathogens that mediate movement of monocytes from blood to tissues during infections. Monocytes differentiate into macrophages during inflammation. Macrophages are then involved in the phagocytosis of pathogens (Geissmann *et al.*, 2010).

1.6.3 Lymphocytes

Lymphocytes are the cells of immune system that form core of adaptive immunity, and specifically recognize and react against foreign antigens. They circulate in blood and lymph and lymphoid organs that are lymph nodes, lymphoid tissues associated with gut, thymus and spleen. Lymphocytes are distinct in their function and divided into two types T lymphocytes, B-lymphocytes and natural killer (NK) cells (Janeway & Medzhitov, 2002).

1.6.4 Platelets

Platelets present in human blood are anucleated, they lack DNA but retain mRNA that are derived from bone marrow megakaryocytes. They have ability for protein translation from cytoplasmic mRNA. Platelets have role in thrombosis, wound repair, vascular remodeling and inflammation (Gnatenko *et al.*, 2003).

1.7 Leukemia

Leukemia is uncontrolled growth of white blood cells (Sahu *et al.*, 2006). Uncontrolled cell division at bone marrow causes accumulation of these abnormal cells in bone marrow,

lymph nodes which interferes with the production of erythrocytes, lymphocytes and platelets that lead to bleeding, anemia and inability to fight infections

1.7.1 Statistics of Leukemia

Leukemia is mostly diagnosed in adults over 20 years of age. The most common type of leukemia among adults is chronic lymphoblastic leukemia CLL, its prevalence is about 36% and AML is 32%. Males are approximately 33% more effected with leukemia than females. Over the past few decades leukemia incidence is increasing. Since 2007 to 2011, an increase of 1.6% in males and of 0.6% in females per year was observed (Siegel *et al.*, 2013)

1.7.2 Classification of Leukemia

On the basis of cell type and growth rate, leukemia is classified into four main types

- Acute lymphocytic leukemia (ALL)
- Chronic lymphocytic leukemia (CLL)
- Acute myeloid leukemia (AML)
- Chronic myeloid leukemia (CML)

1.7.3 Risk Factors Responsible For Leukemia Development

As several causes are attributed to the origin and progression of leukemia, which are carried out in a multi-step process. Ionic radiation is one of the major risk factors causing leukemia except CLL. Family history of patient is a major factor in case of CLL. Cigarette smoke and certain chemicals such as formaldehyde and benzene increase the risk of AML.

1.7.4 Benzene as an Inducer of AML

Benzene, an aromatic compound has been associated with human cancers, e.g., leukemia. Metabolic conversion of benzene leads to production of several phenolic compounds in the body. Principal compounds are phenol, hydroquinone and catechol that are responsible for inducing cytogenetic changes and affect cell cycle (Morimoto & Wolff, 1980).

Benzene and its various metabolites are involved in genetic damage that include structural and chromosomal aberrations in blood and bone marrow of animals and humans that are exposed to it. Benzene may produce genotoxic effects by the generation of reactive oxygen species such as hydrogen peroxide (H₂O₂), hydroxyl radicals (HO[•]), single oxygen (O) in bone marrow. Redox reactions may produce active oxygen that damage cellular DNA phenol, hydroquinone and catechol results in an increased level of oxidative DNA damage. Oxidative DNA damage that results by benzene and its conversion to phenolic compounds play a role in benzene-induced leukemia, myelotoxicity and genotoxicity (Kolachana *et al.*, 1993).

Acute myeloid leukemia caused by benzene exposure is most frequent among all types as previously reported. Chronic myeloid, lymphoid and hairy cell leukemia was also associated with benzene as reported previously (Clavel *et al.*, 1996)

1.7.5 Acute Myeloid Leukemia

Acute myeloid leukemia is characterized as a heritably heterogeneous disease in which certain alterations in somatic cells that interrupt cellular growth, proliferation and differentiation gather in hematopoietic progenitor cells. In case of AML, myeloid cells increase in bone marrow, arrest in their maturing that result in granulocytopenia, thrombocytopenia and anemia, either with or without leukocytosis (Lowenberg *et al.*, 1999).

1.7.5.1 Signs and Symptoms of AML

Sign and symptom of AML are non-specific and diverse but they are directly linked to leukemic intrusion of bone marrow that cause cytopenia. Patients undergo fatigue, infections, fever, hemorrhage because there is reduction in red blood cells, white blood cells and platelets. Leukemic infiltration like hepatomegaly, splenomegaly, lymphadenopathy, bone pain and central nervous system can generate a variety of other symptoms (Lowenberg *et al.*, 1999).

1.7.5.2 Diagnosis of AML

Primary diagnosis of AML occur with the identification of leukemic myeloblasts on the basis of their morphology seen in peripheral blood and bone marrow stained with Wright-Giemsa. Cells have different nucleoli, cytoplasm content very low and nucleus round to irregular. The presence of over 30% blasts in bone marrow is required for definitive diagnosis of AML that distinguish it from other leukemic types.

On the basis of morphological appearance of blasts, AML is divided into 9 subtypes (Bennet *et al.*, 1976; Bennett *et al.*, 1991). Patients with AML have non-random clonal chromosomal aberrations that are identified by cytogenic analysis of leukemic blasts (Rowley, 1980; Yunis, 1984). Diagnosis of AML is now possible by these genetic, immunological and morphological approaches, these approaches not only help to identify subtypes but also provide markers by which patient's response to therapy is monitored (Coco *et al.*, 1992).

1.7.5.3 Treatment of Acute Myeloid Leukemia

Chemotherapy is used to treat many types of leukemia. Evolution of AML classification based on morphology to genetic level of diagnosis is of great importance that is shown by

1.8.1 Rosemary (*Rosmarinus Officinalis*. L)

Rosmarinus officinalis L. commonly known as rosemary is a plant belonging to Labiatae (Lamiaceae) family. Rosemary is an evergreen aromatic shrub whose height reaches to 1.5m (Al Sheyab *et al.*, 2012). Flavonoids such as carnosol, carnosic and rosmarinic acid, and volatile oils are the chemical compounds found in rosemary. Rosemary in extract or ground form is shown to have antioxidant properties because of presence of phenolic compounds (Terpinc *et al.*, 2009).

Rosemary extract has been used on different cancer cell lines including breast, lung, liver, leukemia and prostate (Cheung & Tai, 2007; Yesil-Celiktas *et al.*, 2010). Rosemary extracts showed inhibition of tumorigenesis in rodent models (Moran *et al.*, 2005). Significant anti-proliferation activity has been shown by flavonoids of rosemary extracts against human promyelocytic leukemia HL-60 and B-lineage leukemia cells (Yesil-Celiktas *et al.*, 2010).

1.8.2 *Thymus Vulgaris*

Thymus vulgaris L. commonly known as thyme belong to genus *Thymus* (Lamiaceae family) which is mostly found in the Mediterranean region, Asia, Southern Europe and North Africa. *Thymus vulgaris* extracts have shown immuno-modulating properties (Ocaña & Reglero, 2012) Diverse studies proposed that extracts of *Thymus vulgaris* may have potential anticancer effects. *Thymus* essential oil showed cytotoxicity against cancer cells that may be due to its lipophilic compounds that releases enzymes and metabolites of cancerous cells by accumulating in their cell membranes and increasing their permeability. *Thymus* showed cytotoxic effects on genes taking part in cell cycle, cell death and cancer. The most significantly regulated pathways by thyme essential oil were interferon signaling (cytokines that show potent anti-proliferative, antiviral and immunomodulatory properties),

N-glycan biosynthesis (oligosaccharides that plays role in glycoprotein functions e.g. epidermal growth factor and transforming growth factor- β receptors) and extracellular signal-regulated kinase 5 (ERK5) signaling (involved in regulation of tumor angiogenesis and cell migration and prevents apoptosis (Sertel *et al.*, 2011). Thyme also showed leukocytopoiesis and thrombocytopoiesis. Thymus vulgaris showed anti-leukemic activity in vitro (Von Ardenne & Reitnauer, 1981). It has been shown to have potential selective cytostatic activity in vitro. It is the safest herb that showed least adverse effects (Ayesh & Abed, 2014).

1.8.3 *Ocimum Basilicum*

Basil (family Lamiaceae) is an annual herb used in many kinds of food preparations in Mediterranean diets. Basil is one of the major essential oils producing species belonging to the genus *Ocimum* (Grayer *et al.*, 2002). Its extracts are also used in the manufacturing of cosmetic and pharmaceutical products. Due to phenolic compounds in basil, it showed antitumor, anti-microbial and antioxidant properties Phenolic compounds exhibit redox properties which neutralize free radicals and decompose peroxides (Hussain *et al.*, 2008).

1.9 Mesoporous Silica Nanoparticles (MSNPs)

MSNPs like other inorganic nanoparticles have brought new possibilities in biomedical research as they have numerous striking features for applications as an innovative drug delivery system, such as controllable particle size and shape, large surface areas, tunable pore sizes and exterior and interior (dual) functional surfaces. Controllable size and shape of MSNPs pores can store pharmaceutical drug and control their pre-mature release and degradation before attainment of their destination. Chemotherapeutic agents can be loaded in MSNPs rather than dissolving in solvents that may be hazardous for health. Folic acid attachment to these particles allow targeting of special type of cells such as cancerous cells.

MSNPs are rousing and capable vehicles for various features of biomedical applications (Lu *et al.*, 2010).

1.9.1 Toxicity of MSNPs

Nano toxicology is an emerging discipline in Nano biotechnology. Single and repetitive dose toxicity are two broad things. Repeated dose toxicity is when extended exposure to comparatively low dose toxicant causes harmful effects. Dependent on dose and period of exposure, a solitary compound may cause both acute as well as chronic effects. Repeated dose toxicity studies indicated that mice exposed to MSNPs for 14 days continuously via intravenous administration at 20, 40 and 80 mg/kg presented no death (Liu *et al.*, 2011).

Many factors such as particle size, dose (mass and surface area), surface characteristics (charge, shape, coating etc.) play a key role in toxicity of nanoparticles. Among these, a major role is played by particle size in their contact with biological system (Foster *et al.*, 2001). The ratio between surface area and volume increases as particle decreases in size (Brown *et al.*, 2001).

1.9.2 Tissue Delivery and Excretion of Silica Nanoparticles

Different sized silica nanoparticles (50nm, 100nm and 200nm) were evaluated previously for their toxicity, bio distribution and excretion. It is already reported that 50nm particles were cleared from the body through urine and bile. While 100nm and 200nm particles remained at low concentration as reported through urine and fecal analysis. Silica particles are trapped in liver and spleen by macrophages and remain there until 4 weeks after single injection (Cho *et al.*, 2009).

MSNPs are rousing and capable vehicles for various features of biomedical applications (Lu *et al.*, 2010).

1.9.1 Toxicity of MSNPs

Nano toxicology is an emerging discipline in Nano biotechnology. Single and repetitive dose toxicity are two broad things. Repeated dose toxicity is when extended exposure to comparatively low dose toxicant causes harmful effects. Dependent on dose and period of exposure, a solitary compound may cause both acute as well as chronic effects. Repeated dose toxicity studies indicated that mice exposed to MSNPs for 14 days continuously via intravenous administration at 20, 40 and 80 mg/kg presented no death (Liu *et al.*, 2011).

Many factors such as particle size, dose (mass and surface area), surface characteristics (charge, shape, coating etc.) play a key role in toxicity of nanoparticles. Among these, a major role is played by particle size in their contact with biological system (Foster *et al.*, 2001). The ratio between surface area and volume increases as particle decreases in size (Brown *et al.*, 2001).

1.9.2 Tissue Delivery and Excretion of Silica Nanoparticles

Different sized silica nanoparticles (50nm, 100nm and 200nm) were evaluated previously for their toxicity, bio distribution and excretion. It is already reported that 50nm particles were cleared from the body through urine and bile. While 100nm and 200nm particles remained at low concentration as reported through urine and fecal analysis. Silica particles are trapped in liver and spleen by macrophages and remain there until 4 weeks after single injection (Cho *et al.*, 2009).

1.9.3 Surface Modifications of Mesoporous Silica Nanoparticles for Controlled Drug Release

MSNPs have high surface area and capability to carry drugs. High density of silanol groups are present on silica surface that can be easily modified with a widespread range of organic functional groups. It allows for modification of surface with targeting agents such as antibodies, folic acid, polymers such as cellulose derivatives, polyethylene glycol and many others so that rapid clearance of nanoparticles would occur. These polymers minimize opsonization. Some of the polymers used are described below.

1.9.3.1 Carboxymethyl Cellulose and Ethyl Cellulose

Cellulose derived from plant source is used extensively in pharmaceutical industries. Derivatives of cellulose like ethyl cellulose, carboxymethyl cellulose, methyl cellulose and other are used extensively in oral, topical and injectable formulations. Cellulose is inert and excellent biocompatible element in humans. Carboxymethyl cellulose is used as a primary component of seprafilmTM which is applied to surgical sites for prevention of post-surgical adhesions.

Resins rapidly release the drug as it reaches the target site, therefore they are coated with ethyl or carboxymethyl cellulose to delay drug elution (Jackson *et al.*, 2011).

Immobilization of ethyl cellulose improves the aqueous stability and photo stability of drug (Wilczewska *et al.*, 2012).

1.10 Aims and Objectives

The present study investigates the hematological response elicited by mesoporous hollow core drug coated silica nanoparticles in leukemic rat model.

The main objectives of study were:

- To develop nanoscale drug delivery mechanism in which nanoparticles selectively delivers drug to tumors
- To check the changes in the hematology and morphology of WBCs in leukemic rats after treatment with plant extracts coated MSNP

MATERIALS AND METHODS

2.1 Reagents

Experiment performed deal with the synthesis, characterization of MSNPs, extract loading on MSNPs and targeted delivery of drug in leukemic rats. For the synthesis and loading following reagents are used

Table 1: Chemicals used in MSNPs synthesis and coating.

Name	Formula	Purchase
Carboxymethyl cellulose	CH ₂ CO ₂ H	Sigma-Aldrich
Cetyltrimethylammonium bromide	C ₁₉ H ₄₂ BrN	Sigma-Aldrich
Dimethyl sulfoxide	C ₂ H ₆ OS	Sigma-Aldrich
Sodium Hydroxide	NaOH	Sigma-Aldrich
Starch	C ₆ H ₁₀ O ₅	Sigma-Aldrich
Tetraethyl orthosilicate	SiC ₈ H ₂₀ O ₄	Sigma-Aldrich

2.1.1 Synthesis of Mesoporous Silica Nanoparticles (MSNPs)

MSNPs were synthesized by a chemical method. A 0.25% (w/v) solution of Cetyltrimethylammonium bromide (CTAB) was prepared at 80°C after mixing for 1 h. Tetraethyl orthosilicate (TEOS) (5 mL), a precursor of silica, was mixed drop-wise with 0.25% solution of CTAB. After 2 min incubation at room temperature, solution became turbid showing hydrolysis of silicate which was maintained at stirring for 2 h. Second

solution containing 0.28 % sodium hydroxide (NaOH) was magnetically stirred and heated to 80°C. Both solutions were mixed and kept on stirring overnight. Solution was left until complete settlement of particles. For calcination, filtrate was dried out in oven at 60°C overnight, then temperature was raised to 100 °C for the next 24 h. After complete drying product was collected and made them in fine powder form.

2.2 Characterization of Nanoparticles

MSNP were characterized by XRD (Bruker D8 Advance, Germany), SEM (JEOL JSM-5910) UV-visible spectrophotometer Perkin Elmer UV/VIS-Lambda 25, FTIR (Bruker, Tensor 27).

2.2.1 X-ray Diffraction Spectroscopy

The XRD analysis of MSNPs was done on X-Ray spectrophotometer (Bruker D8 Advance, Germany) using radiation of Cu-K α , $\lambda=1.54$ ° A, at 40 KV and 30 mA. The average particle size was determined from full width and half length (FWHL) using Debye Scherrer equation, $D=0.9\lambda / \beta\cos\theta$

2.2.2 Scanning Electron Microscopy (SEM)

The microscopic features of MSNPs was observed with SEM (JEOL JSM-5910). To observe genuine pore structures on the external surface, the samples were observed without any metal coating for SEM. By using a low accelerating voltage, we can obtain selective information from the surface region.

2.2.3 UV- VIS Spectroscopy

The optical absorption spectra of uncoated MSNPs, drug loaded MSNPs and polymers were measured by UV-VIS spectrophotometer (Perkin Elmer UV/VIS-Lambda 25). Absorption spectra were taken in the range of 250-800nm at room temperature.

2.2.4 Fourier Transform Infrared Spectrophotometer (FTIR)

Dried powder of each plant extract was used for FTIR analysis. Powder (10 mg) of the dried extract was encapsulated in 100 mg of KBr pellet, in order to prepare translucent sample discs. The powdered sample of each plant extract was loaded in FTIR spectroscope (Bruker, Tensor 27) with a scan range from 400 to 4000 cm^{-1} with a resolution of 4 cm^{-1} .

2.3 Collection of Plant Material

Plant material was collected from clonal repository of National Agriculture Research Center (NARC) Islamabad.

2.4 Drug Loading on Nanoparticles

After synthesis of MSNPs, methanolic plant extracts (*Rosmarinus officinalis*, *Thymus vulgaris* and *Ocimum basilicum*) were loaded on them. Plant extract (0.9 g) was dissolved in 5 mL ethanol. The solution was sonicated until extract was completely dissolved. MSNPs (0.18 g) were mixed with drug solution and incubated overnight. The solution was air dried and mashed to get powder form.

2.5 Polymer Coating on Extract-Loaded Silica Nanoparticles

2.5.1 Ethyl Cellulose Coating on Thymus Vulgaris Loaded MSNPs

TH-loaded MSNPs were completely dissolved in 4.1 mL dimethyl sulfoxide (DMSO) i.e. conjugate solution (MSNPs + extract). Polymer solution was made by dissolving 0.009 g ethyl cellulose in 5 mL DMSO. These solutions were mixed and incubated at room temperature on magnetic stirrer for 2 h. Product was sealed to avoid contamination.

2.5.2 Carboxymethyl Cellulose (CMC) Coating on Ocimum Basilicum-Loaded MSNPs

To coat CMC on Ba, 0.009g CMC was dissolved in 5mL DMSO. Another solution was made by dissolving 0.008g of drug loaded MSNPs in 4.1 mL DMSO. Both solutions were mixed while stirring for 2 h and sealed to avoid contamination.

2.5.3 Soluble Starch Coating on Rosmarinus Officinalis (RM)-Loaded MSNPs

RM-loaded MSNPs were coated by soluble starch. RM-loaded MSNPs (0.008 g) were dissolved in 4.1 mL DMSO. Soluble starch (0.009 g) was dissolved in 5mL DMSO. Both solutions were mixed and incubated on magnetic stirrer for 2 h. The final solution was sealed to avoid contamination.

2.6 In Vivo Studies

Male rats (6-8 weeks old) of genus *Sprague Dawley* were purchased from NIH (National Institute of Health) laboratories and maintained at animal house facility at Quaid-i-Azam University. Rats were fed properly and given filtered water and maintained in a temperature controlled room. Animals were housed as 1/cage. All the procedures were done as recommended by the Ethical Committee of Quaid-i-Azam University to handle animals (BEC-FBS-QAU-09).

2.6.1 Benzene Studies

Benzene dissolved in isopropanol (IPA) and injection water was used for all studies. Benzene, injection water and isopropanol were taken according to a ratio of 1.5:1.5:2. Time course studies were performed using a dose (0.1mL/day/rat) of benzene administered to 4 groups of rats (3 experiments/3 rats/ group). Each group had corresponding simultaneous

controls (3/3 rats/group). Dose response studies were conducted using one group of rats (3/3 rats/group) and the rest of three groups were used for treatment after administration of benzene for 3 weeks which were corresponding to 9 doses of benzene. Benzene dose (0.1 mL) was administered at alternate days.

2.6.2 Drug Administration

Out of 4 groups (3 rats/group) which have been given benzene doses, 3 groups were subjected to treatment. Final form of MSNPs (extracts + polymer coated) were given in dose dependent manner (0.1 mL/day/rat). Three different groups were given separate drugs, rosemary-loaded MSNPs to group 3, thymus-loaded MSNPs to group 4 and basil-loaded MSNPs to group 5.

2.7 Blood Profiling of Rats

A drop of blood from rat's tail was layered onto the slide. A thin smear was made. Blood profiling was done as per schedule shown in figure 1. Group I represented normal rats that are taken as control. They were left untreated. Group II represented benzene treated rats, given benzene intravenously for three weeks. Group III showed RM-loaded MSNPs treated rats. After benzene injection for 2 weeks treatment was started and 9 doses of RM-loaded MSNPs were given. In Group IV leukemia was induced by benzene administration and then treated with TH- loaded MSNPs. Group V showed rats treated with Ba-loaded MSNPs after leukemia induction by the action of benzene.

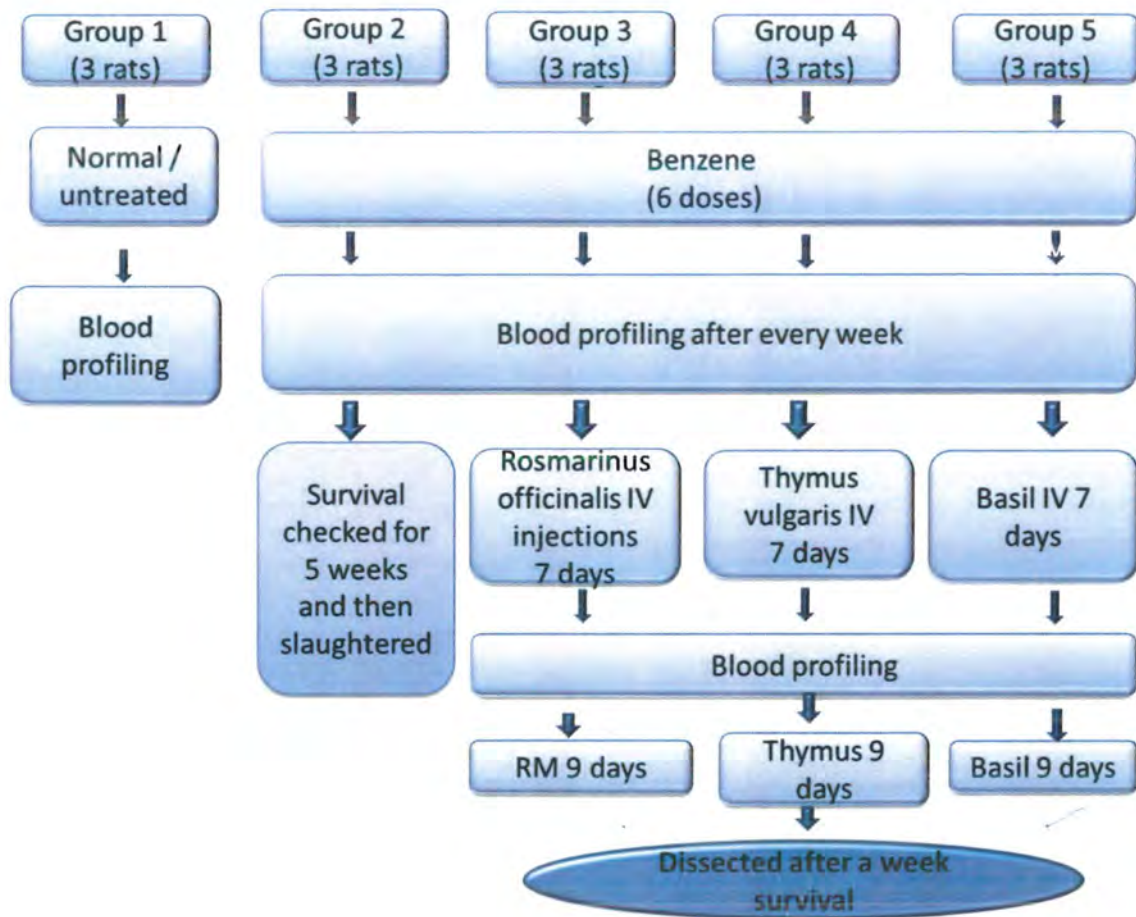


Figure 1: Schematic representation of leukemia induction and treatment with extract-loaded MSNPs in 5 groups of rats.

2.8 Giemsa Staining

Table 2: Reagents used in leukemia induction and blood cells staining

Name	Formula	Purchase
Benzene	C ₆ H ₆	Merck
Giemsa		Sigma
Methanol	CH ₃ OH	Merck
Isopropanol	C ₃ H ₈ O	Merck

2.8.1 Blood Smear Formation

Rats of each group were anesthetized and opened by mid abdominal incision. Blood was taken from heart and collected immediately in EDTA tubes and impression smears were made on slides. After drying, cells were fixed in absolute methanol for 10 min and stained with Giemsa dye (MAK, Country) (10X dilution of Giemsa in PBS). Slides were examined under light microscope (IRMECO) for morphological analysis and differential count of rat blood cells.

2.8.2 Bone Marrow Staining

After sacrificing rats their bone marrow was collected from femur and tibias by flushing shaft with PBS using a syringe with a needle 26G. Gentle pipetting was done to avoid disaggregation. Cells were centrifuged at 200g for 10 min and supernatant was discarded. The cell pellet was re-suspended in PBS. Bone marrow cells were fixed on slide, stained with Giemsa dye and morphological studies were done under light microscope (IRMECO, X100).

Results

3.1 Characterization of MSNPs

Characterization of synthesized MSNPs was done by means of XRD, SEM, UV-VIS spectroscopy and FTIR spectroscopy.

3.1.1 Particle Size and Shape Analysis

XRD analysis of MSNPs was done on X-ray spectrophotometer (Shimadzo 6000) by using radiations of Cu-K α , $\lambda=1.54\text{\AA}$, at current of 30 mA and voltage of 40K. Fig 2 represents the XRD pattern of MSNPs. The observed pattern showed diffraction peak at $2\theta=31.035$. Size was determined from Full Width at Half Maximum (FWHM) using Debye Scherrer equation, $D=0.9\lambda/\beta\cos\theta$ that showed MSNPs are of 47.94nm diameter.

Table 3: Calculation of MSNPs diameter from Scherrer equation.

K	0.9
λ	1.54E-10
$k\lambda$	1.4E-10
Sample	SiO ₂
β Obs	0.03
2θ	31.03
θ	15.5
Θ (Radian)	0.27
$\text{Cos}\theta$	0.96
$\beta.\text{Cos}\theta$	0.028
D	4.8E-09
D(nm)	47.94

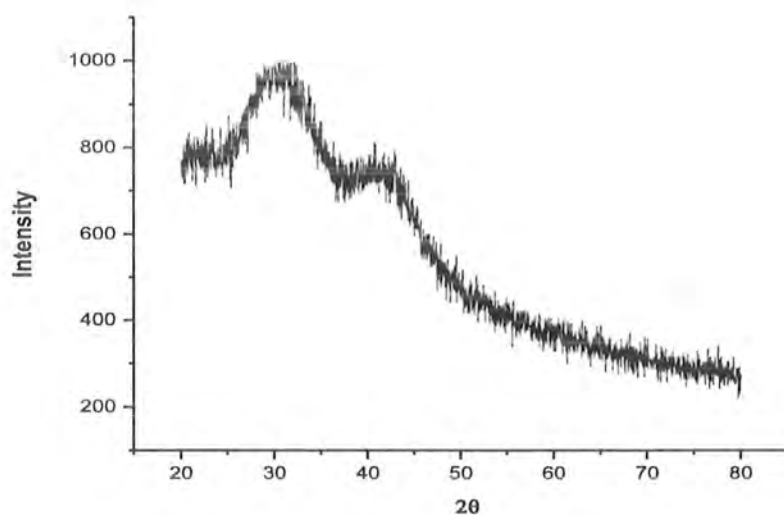


Figure 2: XRD Pattern of MSNPs.

3.1.2 Scanning Electron Microscopy (SEM)

Microscopic features of MSNPs were observed by SEM. To observe genuine pore structures on external surface, MSNPs were observed without any coating for SEM. Figure 3 shows SEM images taken at different resolutions. This SEM confirms mesoporous nature of MSNPs and size calculated by XRD.

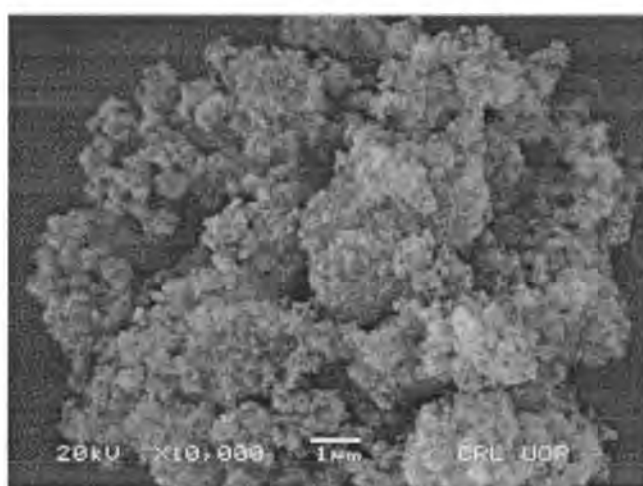


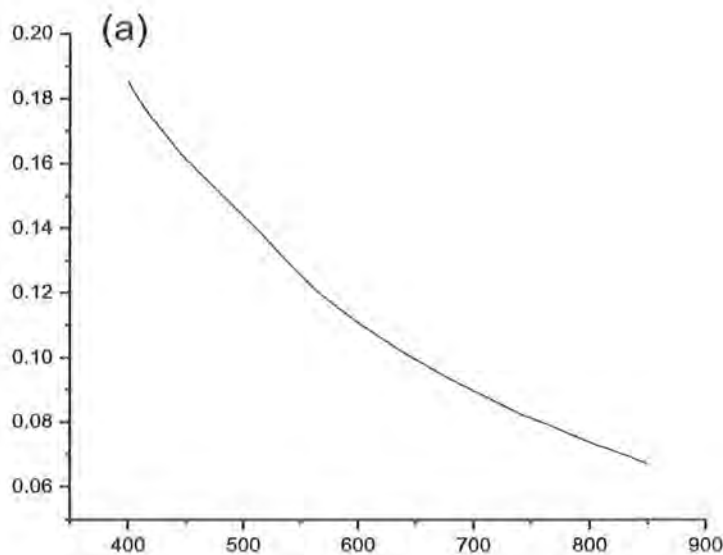
Figure 3: SEM of MSNPs.

3.1.3 Spectrophotometric Analysis

The optical absorbance spectra of nanoparticles were measured by UV/Vis in liquid cuvette configuration. Absorption spectra was taken at room temperature over range of 200-800nm.

3.1.3.1 UV-VIS Spectroscopy Of MSNPs, Crude Extract and Extract Loaded MSNPs

Figure 4(a) show the absorbance spectra of MSNPs. MSNPs showed no absorbance in visible region. The absorbance pattern of RM crude extract (4b) and RM-loaded MSNPs exhibited characteristic absorption at 680nm. Figure 4(c) represent absorbance of TH and 4(d) TH-loaded MSNPs, both of the samples displayed absorption spectra at 670nm. Ba crude extract (figure 4e) and Ba-loaded MSNPs (figure 4f) showed absorbance at 410 and 670nm showing no other peak. This data confirmed loading of all plant extracts on MSNPs as they showed same absorbance pattern observed in crude extracts.



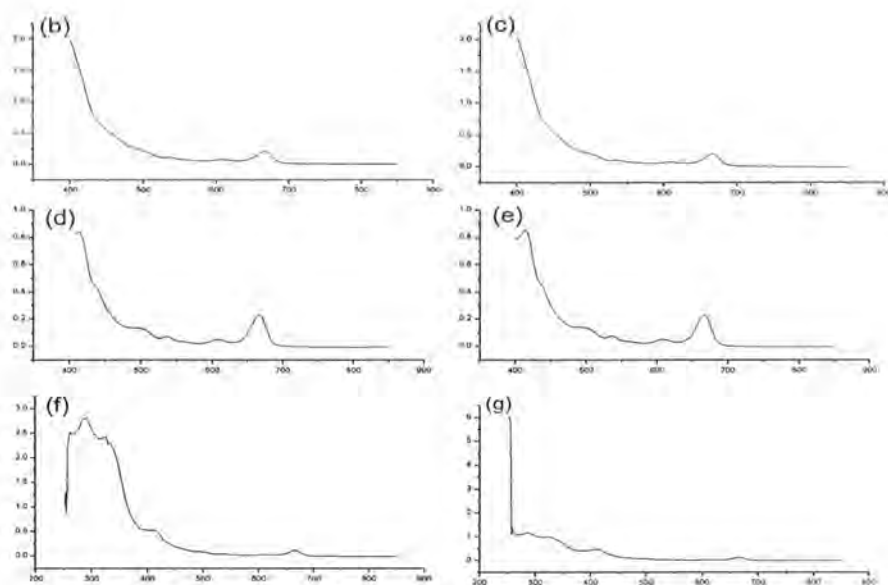


Figure 4: Absorbance spectra of MSNPs, crude extracts and extract loaded MSNPs. (a), MSNPs; (b) RM crude extract; (c), RM-loaded MSNPs; (d) TH crude extract;(e), TH-loaded MSNPs; (f), Ba crude extract; (g), Ba-loaded MSNPs.

3.1.4 FTIR- Spectroscopy

3.1.4.1 RM Coated MSNPs Encapsulated by Starch

Absorbance spectra of MSNPs (a), RM (b), RM coated MSNPs, starch (d) and final form of MSNPs loaded with drug and encapsulated in starch (e) is shown. Characteristic peaks are shown in ranges of $550\text{--}850\text{ cm}^{-1}$ shows presence of alkyl halide. $1000\text{--}650$ shows alkenes are there. $1000\text{--}1320\text{ cm}^{-1}$ that represent alcohols, carboxylic acids, esters, ethers are present $1250\text{--}1020\text{ cm}^{-1}$ shows aliphatic amines. Peak in range $1470\text{--}1450\text{ cm}^{-1}$ that shows alkanes are present. Peak in range $1550\text{--}1475$ depicts presence of nitro compounds. Peak lying in range $1650\text{--}1580$ shows the presence of primary amines. $2260\text{--}2100$ shows alkynes. Alkanes are present as peak range is between $3000\text{--}2850$. Peak lying in 3400--

3250 that depicts presence of primary, secondary amines, amides. 3100–3000 shows alkynes are present.

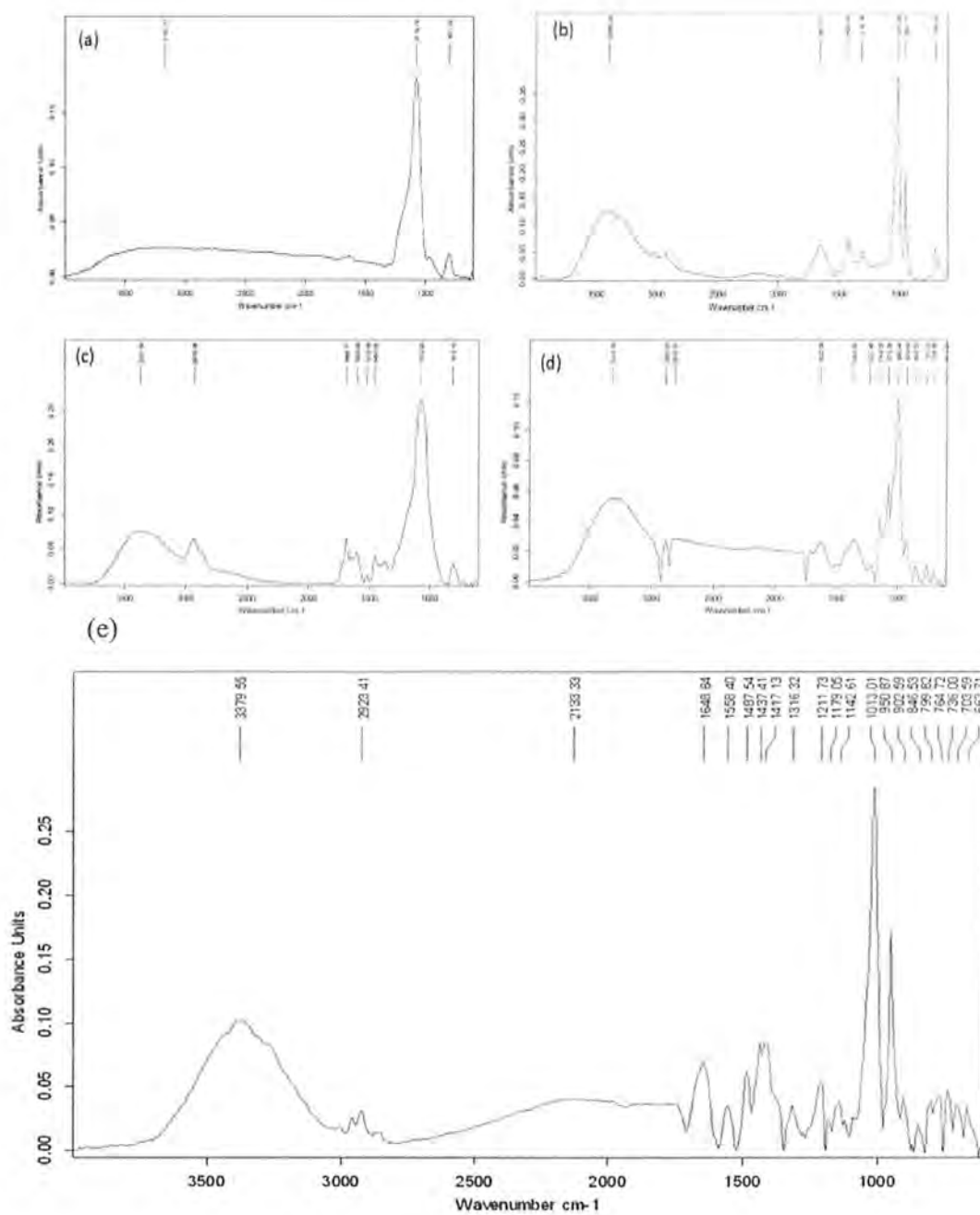
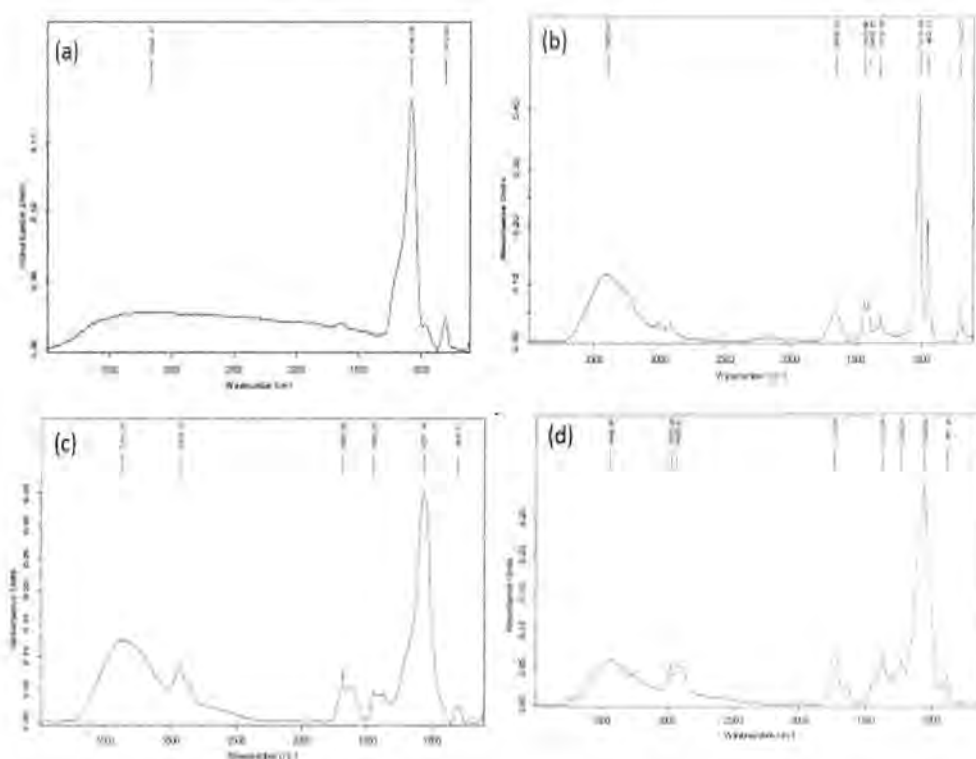


Figure 5: FTIR of RM-loaded MSNPs with soluble starch coating. (a) MSNPs; (b) RM crude extract; (c) RM coated MSNPs; (d) soluble starch; (e) final loading product MSNPs, RM and soluble starch.

3.1.4.2 TH-loaded MSNPs coated by EC

Absorbance spectra of MSNPs shown in figure 6(a), thymus crude extract (figure 6b), TH-loaded MSNPs (6c), ethyl cellulose (EC) (6d) and final form of MSNPs loaded with TH and coated with ethyl cellulose (6e). Characteristic peaks are shown in ranges of 550–850 cm^{-1} shows presence of alkyl halide. 900–675 cm^{-1} shows aromatics are there. 1000–650 cm^{-1} shows alkenes are there. 1000–1320 cm^{-1} that represent alcohols, carboxylic acids, esters, ethers are present. 1250–1020 cm^{-1} shows aliphatic amines. 1360–1290 shows nitro compounds in this group. Peak in range 1550–1475 depicts presence of nitro compounds. 1680–1640 cm^{-1} shows presence of alkenes. 2260–2100 cm^{-1} shows alkynes. Alkanes are present as peak range is between 3000–2850. Peak lying in 3400–3250 that depicts presence of primary, secondary amines, amides. 3100–3000 shows alkynes are present. 3500–3200 shows phenols and alcohols are there.



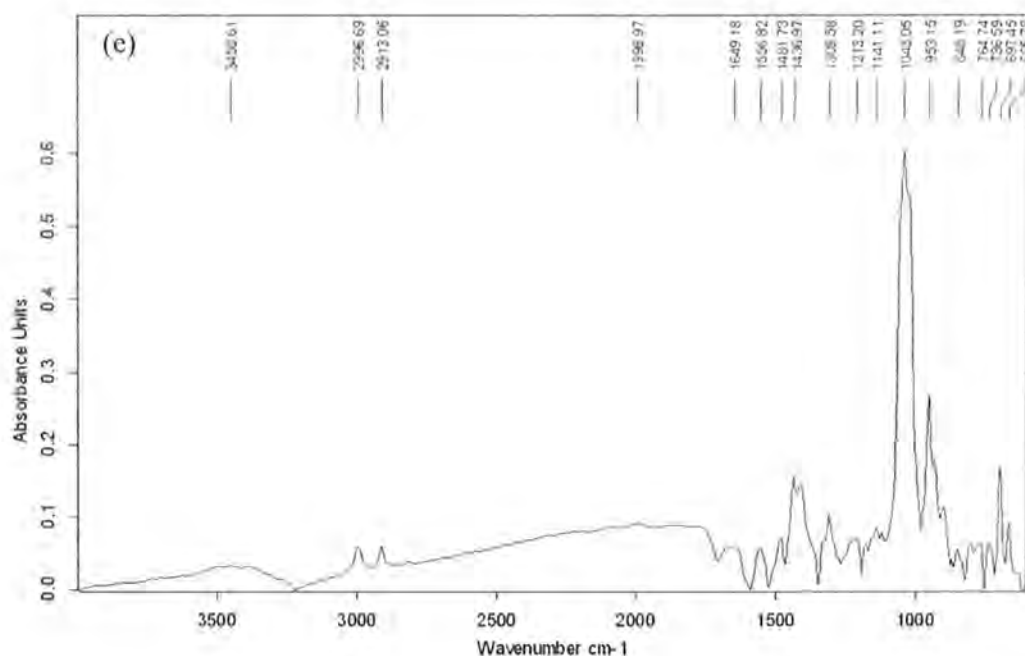


Figure 6: FTIR of TH-loaded MSNPs with EC coatings. (a) MSNPs; (b) TH crude extract; (c) TH-loaded MSNPs; (d) EC; (e) final loading product MSNPs, TH and EC.

3.1.4.3 FTIR of Ba-loaded MSNPs with CMC Coatings

IR spectra is represented in figure 7, MSNPs (7a), basil crude extract (7b), Ba-loaded MSNPs (7c), starch (7d) and Ba-loaded MSNPs encapsulated with CMC (e). Peaks observed in all these loading are between ranges of 550-850 cm^{-1} shows presence of alkyl halide. 650-1000 cm^{-1} that shows alkenes. 1000-1320 cm^{-1} that represent alcohols, carboxylic acids, esters, ethers are present. 1250-1020 cm^{-1} shows aliphatic amines are found in this compound. 1500-1400 that shows aromatic groups are present. 1475-1550 shows presence of nitro compounds. 1710-1665 that shows alpha, beta-unsaturated aldehydes, ketones are present. 2260-2100 shows alkynes. 3000-2850 that shows alkanes are present. 3200-3500 that shows alcohols and phenols are there in this compound.

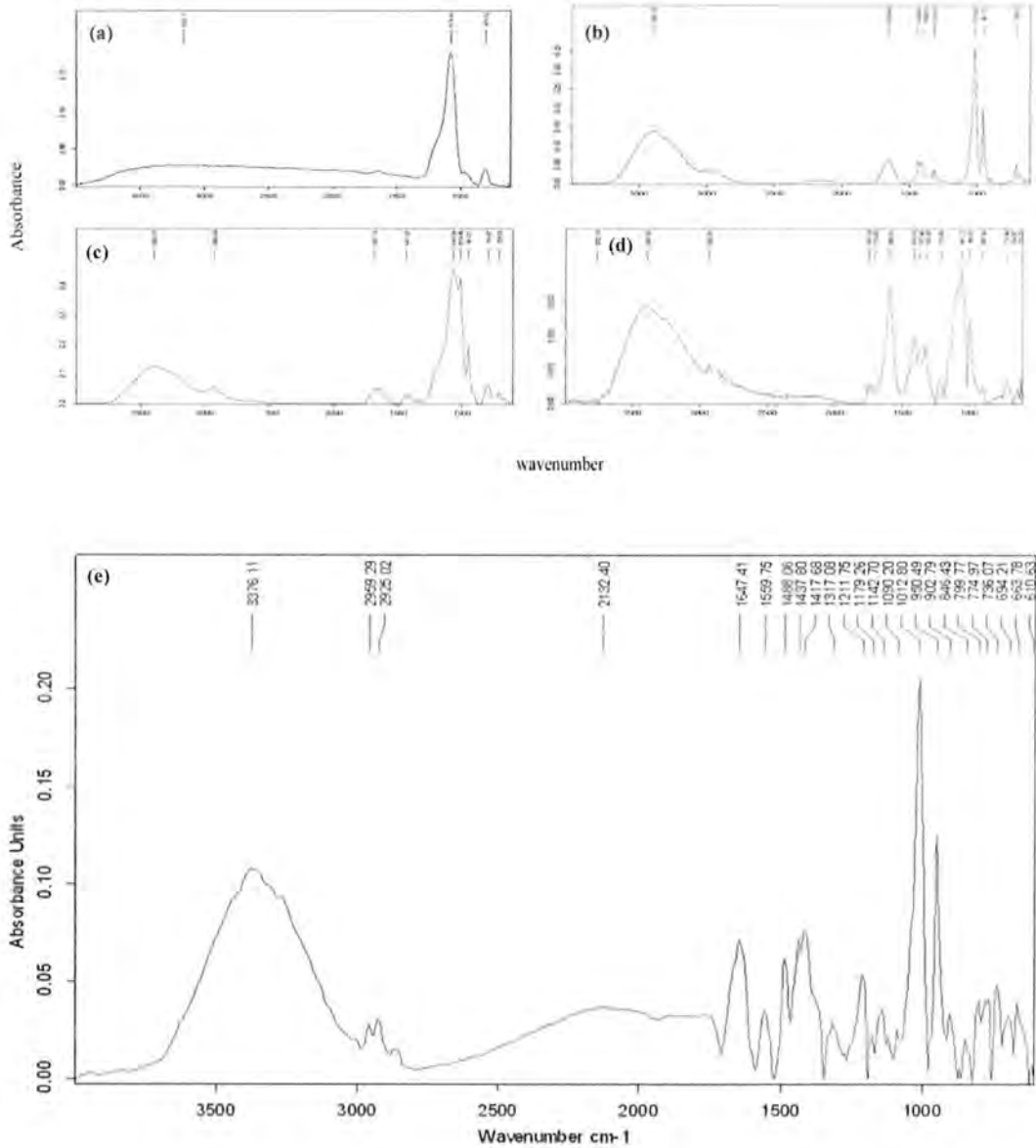


Figure 7: FTIR of Ba-loaded MSNPs with CMC coatings. (a) MSNPs; (b) Ba crude extract; (c) Ba-loaded MSNPs; (d) CMC ; (e) final loading product MSNPs, basil and CMC.

3.2 Relative Organ Weight of Control, Leukemic and Treated Groups of Rats

Body weight of rats were measured initially, after benzene treatment and finally at the time of dissection after treatment with nanomedicines. Average body and organ weights of rats from all groups was calculated and shown in figure. Control represents group I rats that were normal without any treatment and taken as a reference to compare other groups. Leukemic rats represent group II that were induced leukemia by benzene dosing. RM shows group III that was *Rosmarinus officinalis* coated MSNPs treated group. TH represents group IV that is *thymus vulgaris* coated MSNPs treated group. Ba represents group V that is treated by basil coated MSNPs. Examining the relative body weight of organs from all groups showed significant decrease in liver weight of TH group. No significant change in the relative body weights of other organs was observed.

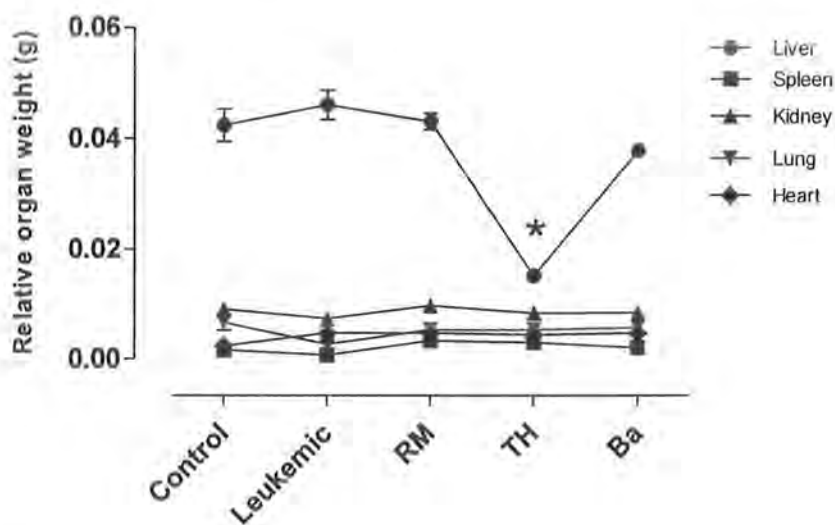


Figure 8: Comparison of relative organs weight of control, leukemic and treated groups of rats.

3.3 Hematological Profile of Normal, Leukemic and Treated Rats

3.3.1 Comparison of WBCs Differential Count of Control Vs Leukemic Group

To see the differential count of rats, blood smears were made on microscopic glass slides and stained with giemsa dye. Average white blood cell count of group I rats showed 6% neutrophils, 67% lymphocytes, 8% monocytes, 0.8% eosinophils, and 2.9% basophils. Group II rats were administered benzene intravenously and blood profiling was done after 1, 2 and 3 weeks of injection. 1st week of benzene injection showed 14% neutrophils, 57% lymphocytes, 8% monocytes, 1% eosinophils. 2nd week of benzene showed increase of neutrophils up to 40%. Lymphocytes decreased to about 38%, monocytes 4%. Significant increase was found in neutrophils and significant decrease in lymphocytes. Significant (*) increase was seen in W2 neutrophil count and significant decrease shown in lymphocytes of W2. 3rd week data is not shown here as most of the cells were burst and damaged by benzene action.

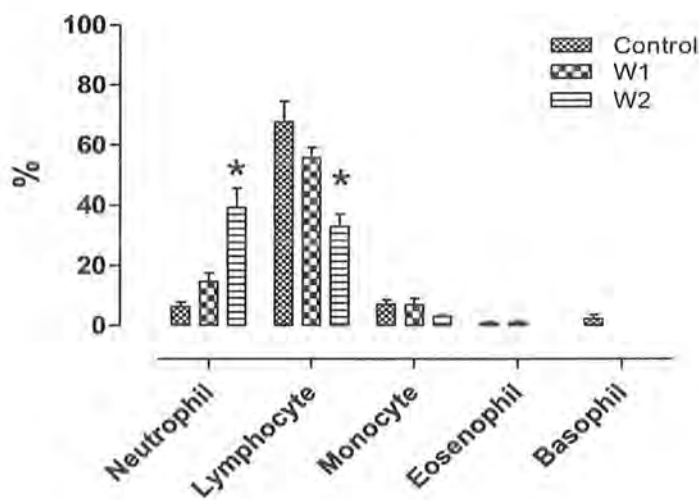


Figure 9: Differential count of WBCs in rats induced with benzene. Control; (W1) week 1 and (W2) after benzene administration.

3.2.2 Comparison of WBCs Differential Count of Leukemic Vs Treated Groups

Average count of WBCs stained with giemsa in leukemic rat (W2) after two weeks of benzene administration showed neutrophils 40%, lymphocytes 38%, and monocytes 4%. Group III (treated with RM-loaded MSNPs) showed 16% neutrophils, 23% lymphocytes, 4% monocytes, 1% eosinophils, and 3% basophils. Group IV (treated by thymus-loaded MSNPs) showed 36% neutrophils, 10% lymphocytes, 14% monocytes, 0.5% eosinophils and 0.7% basophils. Group V (basil loaded MSNPs treated) rats showed average neutrophil count of 9%, 35% lymphocytes, 4% monocytes, eosinophils 2% and 2.5% basophils. W2 / RM exhibited significant decrease in neutrophil count. W2/TH showed significant decrease in lymphocytes and significant increase in monocyte count. W2/Ba shows significant decrease in neutrophil count.

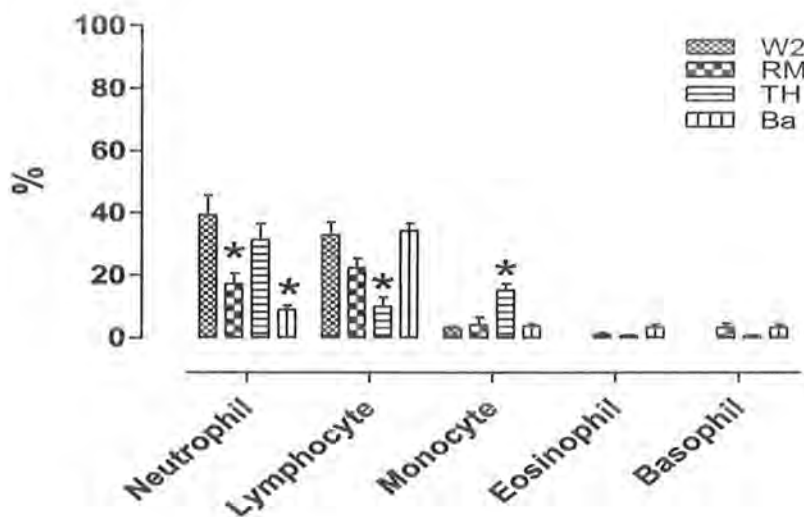


Figure 10: Differential count of WBCs in rats after benzene administration and treatment with extract-loaded MSNPs. W2 shows (week 2 of benzene); RM, (*Rosmarinus officinalis* loaded MSNPs); TH, (*thymus vulgaris* loaded MSNPs) and Ba (*Ocimum basilicum* loaded MSNPs).

3.3 Microscopic Examination of Blood Cells

Blood smear were made on glass slides and after methanol fixation stained with Wright-Giemsa Dye and studied under microscope. Following images shows morphology of blood cells and BM.

3.3.1 Bone Marrow

Bone marrow analysis under microscope 100X objective stained with giemsa showed distinction between control, leukemic and treated groups. BM of normal rat (11a) showed erythrocytes (Er), myeloid cells (M), non-segmented neutrophils (NSN), segmented neutrophils (SN) and pro-myelocytes (P) and myeloblasts (MB). Leukemia treated rats (figure 11b) showed myeloblasts (MB), pro-myelocyte (P), late myelocytes (M), non-segmented neutrophil (NSN), segmented neutrophils (SN) and erythroid precursors (Er). Large number of blast cells and mature lymphocytes were seen in leukemic rat. Figure 11(c) showed BM of RM-loaded MSNPs treated group. Red blood cell precursors were more prominent and granulated cell's precursors were also seen. TH-loaded MSNPs showed BM with fat bodies prominent and less blast cells were found as shown in figure 11(d). BM analysis showed more neutrophil precursors in this group. Figure 11 (e) represent BM of Ba-loaded MSNPs treated group. WBCs precursors were seen along with erythrocyte precursors with less no of blast cells.

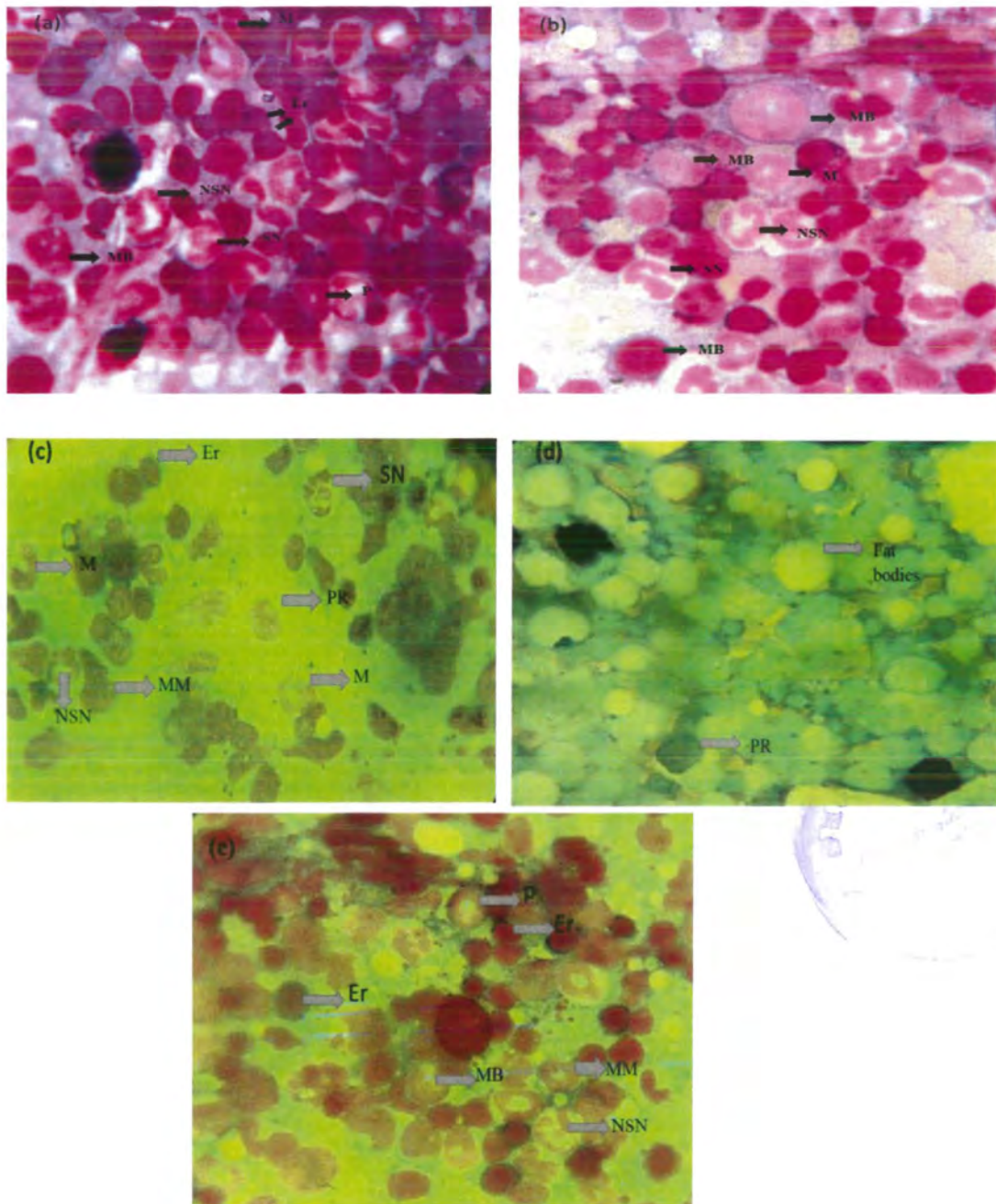


Figure 11: Bone Marrow of normal, leukemic and treated rats. (a), control BM; (b) benzene treated; (c), RM-loaded MSNPs; (d), TH-loaded MSNPs; (e), Ba-loaded MSNPs treated. Where MB indicates myeloblasts; P, pro-myelocyte; M, late myelocyte; NSN, non-segmented neutrophil (band); SN, segmented neutrophil; Er, erythroid precursor.

3.3.2 Erythrophagocytosis Shown by Leukemic Rats

Microscopic examination of giemsa stained blood smear of leukemic rats showed erythrophagocytosis. Figure 12 represent this phenomenon where WBCs engulfed erythrocytes.

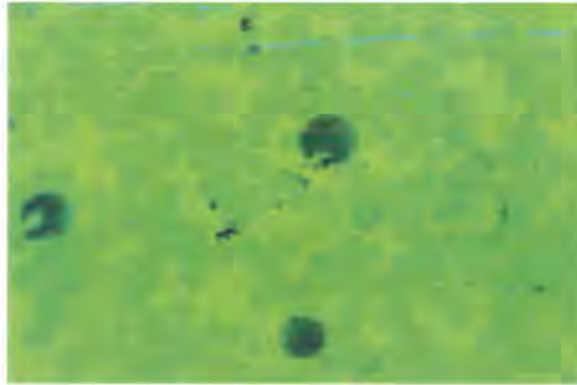


Figure 12: Erythrophagocytosis shown by leukemic rat.

3.3.3 Blood Cells Morphology

Blood was taken from rats and smear was made and stained with giemsa. Microscopic examination with X100 showed morphology changes of red blood cells as well as white blood cells depending on the type of treatment. Fig (a) represents normal group of rats in which RBCs as well as WBCs are intact with their regular shape. (b) Is representing blood cells morphology of leukemic rat, WBCs seemed to be burst with different shapes as compared to normal cells. (c) Represents RM treated group, RBCs were of regular shape and WBCs with real morphology was seen in blood stream. (d) Characterizes thymus coated MSNPs treated rat blood, both RBCs and WBCs with intact shape were seen. (d) Signify basil coated MSNPs treated blood, RBCs regained their form and WBCs were also seen in definite morphology.

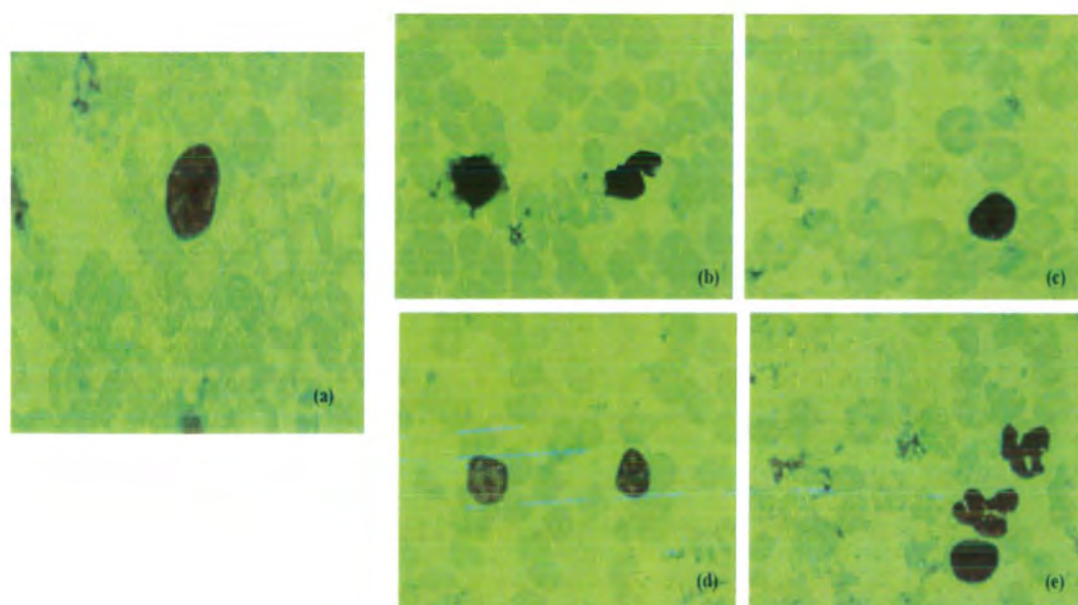


Figure 13: Blood cells morphology. (a) , Normal; (b), benzene treated; (c) RM-loaded MSNPs; (d), TH-loaded MSNPs ; (e), Ba-loaded MSNPs treated rats.

Discussion

Nano-medicine has opened new avenues for improving therapeutical and pharmacological effects of conventional drugs. Nanoparticles due to their small size and large surface area proved to be beneficial in targeted drug delivery. Nanoparticles reach cellular level and can cross blood brain barrier due to their small dimensions. Site specific targeting allows less damage to normal tissues as it delivers drug to pathological site.

MSNPs have high capacity of drug loading, better *in vitro* and *in vivo* biocompatibility and can be excreted safely from the body. MSNPs characterized through XRD, UV/VIS spectroscopy, SEM and FTIR confirmed the final formulation of MSNPs. It is already established that anti-tumor drug loaded nanoparticles of less than 50 nm size show target specificity (Zhang *et al.*, 2014). XRD and SEM analysis of MSNPs confirmed size of 47.9 nm which corresponds to the previously published data. FTIR data (1076 cm^{-1} and 3162 cm^{-1}) confirmed the presence of Si-O and silanol O-H stretching which are the characteristic bonds of MSNPs and corresponds to the data published elsewhere (Mondal & Mishra, 2014).

Three different plant crude extracts (rosemary, thymus and basil) were loaded on MSNPs. The quantity of extract loaded on MSNPs was set as 150mg/kg body weight of rat (unpublished data). MSNPs were taken according to 20mg/kg of body weight of rats. It is already reported that dosage (50mg/kg body weight) of MSNPs is adequate for *in vivo* or *in vitro* application in cancer therapy (Lu *et al.*, 2010).

Silicon nanoparticles are decomposed to soluble ortho-silicic acid and purged through renal system of the body within four weeks. When intravenously administered, these particles accumulate in liver, kidneys and spleen. Authors demonstrated that silica nanoparticles are safely excreted through renal route even if they are not delivered to the target site (Slowing

et al., 2008). MSNPs showed no considerable toxicity (data not shown) to organs and their growth was same as that of control.

Extract loading on MSNPs was confirmed by UV/Vis spectrophotometric data analysis and FTIR spectra. Characteristic peaks of SiO₂ and loaded extracts were seen on final formulation of MSNPs. This confirmed quality of loading on MSNPs. Extract-loaded MSNPs were coated with different polymers which made them sustained-release formulation. FTIR data also confirmed the presence of polymers on the surface of MSNPs. Starch has been reported to be used as a stabilizer or suspending aid of insoluble particles in aqueous media (Božanić *et al.*, 2007). The coated polymers were biocompatible. These polymers delay the abrupt release of drug from the MSNPs. The sustained release strategy was applied so that maximum drug should reach target cells causing least damage to normal cells.

Extract-loaded MSNPs were evaluated for their potential for symptomatic improvement of AML. Benzene, a potent inducer of AML, administration for two weeks showed increased leukocyte count in the blood smear. Neutrophilia, lymphopenia and decreased level of monocytes were observed in addition to presence of blast cells in blood smear that confirmed AML. Lymphopenia during AML might be due to the elevated level of plasma arginase-II which halts T-cell proliferation. Blast cells in BM polarize surrounding monocytes to an immunosuppressive M-2 like phenotype that is also dependent on arginase (Mussai *et al.*, 2013). This also results in low count of monocytes. BM analysis showed higher number of blast cells in leukemic rats as compared to the control BM.

After three weeks of benzene administration, leukocytes were disrupted or distorted and BM had higher number of blast cells. Treatment after three weeks of AML induction showed no significant improvement that might be due to severity of disease. Hence,

treatment was started after second week of AML induction that showed improvement in AML condition.

RM-loaded MSNPs showed decrease in neutrophils and lymphocytes counts as compared to diseased blood profile of same rat group. Relative weight of different organs in rats treated with RM-loaded MSNPs was almost same as compared to control with slight deviations.

TH-loaded MSNPs treatment did not show significant decrease in neutrophil count. However, significant decrease in lymphocytes count was observed as a reaction of this treatment. Monocyte count was significantly increased by the action of *Thymus vulgaris*. Relative weight of different organs was normal except the liver which showed significant decrease after treatment relative to control and benzene treated. TH-loaded MSNPs did not show considerable improvement in morphology of hematology AML rats.

Differential count after treatment with Ba-loaded MSNPs showed significant decrease in neutrophil count which improved up to normal level. Lymphocytes count was in normal range and monocytes count was decreased. Among three formulations of MSNPs, Ba-loaded MSNPs showed significant improvements in AML condition. Our data corresponds to the previous finding where *Ocimum basilicum* exhibits significant activity against benzene-induced hematotoxicity in mice (Saha *et al.*, 2012).

The BM of benzene treated rats showed higher number of blast cells as compared to the BM of control and extract-loaded MSNPs treated rats. However, information of types of niches in the BM which coordinate in hematopoiesis and what are effects of benzene on them is still lacking (Snyder, 2012).

It is concluded that generic MSNPs showed characteristic physical properties which are suited to their usage as drug carriers. Rosemary, Thymus and Basil loaded MSNPs

exhibited a capacity to minimize the impact of benzene (AML condition) as seen by differential count of WBC, relative organ weight analysis, morphological analysis and BM analysis. However, Ba-loaded MSNPs exhibited significant impact to improve cellular indicators as compared to RM- and TH-loaded MSNPs.

FUTURE PERSPECTIVE

The data warrants further investigation to assess the mechanistic pathway of AML induction. Moreover, impact of prescribed plants extracts as nano-medicine might be investigated through expression of arginase-II, TNF- α and relevant pro-inflammatory cytokines as these markers are elevated during AML.

References

- Al Sheyab FM, Abuharfeil N, Salloum L, Hani RB, Awad DS (2012). The effect of Rosemary (*Rosmarinus officinalis*. L) plant extracts on the Immune response and lipid profile in mice. *Journal of Biology and Life Science* 3(1)
- Allen TM, Cullis PR (2004). Drug delivery systems: entering the mainstream. *Science* 303(5665): 1818-1822
- Arruebo M, Fernández-Pacheco R, Ibarra MR, Santamaría J (2007). Magnetic nanoparticles for drug delivery. *Nano today* 2(3): 22-32
- Ayesh BM, Abed AA (2014). In vitro inhibition of human leukemia THP-1 cells by *Origanum syriacum* L. and *Thymus vulgaris* L. extracts. *BMC research notes* 7(1): 612
- Barnes CA, Elsaesser A, Arkusz J, Smok A, Palus J, Lesniak A, Salvati A, Hanrahan JP, Jong WHd, Dziubałtowska E (2008). Reproducible comet assay of amorphous silica nanoparticles detects no genotoxicity. *Nano Letters* 8(9): 3069-3074
- Bennet J, Catovsky D, Daniel M-T, Flandrin G, Galton D, Gralnick Ht, Sultan C (1976). Proposals for the classification of the acute leukemias. *Br J Haematol* 33(4): 451-458
- Bennett J, Catovsky D, Daniel MT, Flandrin G, Galton D, Gralnick H, Sultan C (1991). Proposal for the recognition of minimally differentiated acute myeloid leukaemia (AML-MO). *British journal of haematology* 78(3): 325-329
- Božanić D, Djoković V, Blanuša J, Nair P, Georges M, Radhakrishnan T (2007). Preparation and properties of nano-sized Ag and Ag₂S particles in biopolymer matrix. *The European Physical Journal E* 22(1): 51-59

- Brown DM, Wilson MR, MacNee W, Stone V, Donaldson K (2001). Size-dependent proinflammatory effects of ultrafine polystyrene particles: a role for surface area and oxidative stress in the enhanced activity of ultrafines. *Toxicology and applied pharmacology* 175(3): 191-199
- Chang J-S, Chang KLB, Hwang D-F, Kong Z-L (2007). In vitro cytotoxicity of silica nanoparticles at high concentrations strongly depends on the metabolic activity type of the cell line. *Environmental Science & Technology* 41(6): 2064-2068
- Che S, Lund K, Tatsumi T, Iijima S, Joo SH, Ryoo R, Terasaki O (2003). Direct Observation of 3D Mesoporous Structure by Scanning Electron Microscopy (SEM): SBA-15 Silica and CMK-5 Carbon. *Angewandte Chemie International Edition* 42(19): 2182-2185
- Cheung S, Tai J (2007). Anti-proliferative and antioxidant properties of rosemary *Rosmarinus officinalis*. *Oncology reports* 17(6): 1525-1531
- Cho K, Wang X, Nie S, Shin DM (2008). Therapeutic nanoparticles for drug delivery in cancer. *Clinical cancer research* 14(5): 1310-1316
- Cho M, Cho W-S, Choi M, Kim SJ, Han BS, Kim SH, Kim HO, Sheen YY, Jeong J (2009). The impact of size on tissue distribution and elimination by single intravenous injection of silica nanoparticles. *Toxicology letters* 189(3): 177-183
- Clavel J, Conso F, Limasset J, Mandereau L, Roche P, Flandrin G, Hémon D (1996). Hairy cell leukaemia and occupational exposure to benzene. *Occupational and Environmental Medicine* 53(8): 533-539
- Coco FL, Diverio D, Avvisati G, Arcese W, Petti M, Meloni G, Mandelli F, Pandolfi P, Grignani F, Pelicci P (1992). Molecular evaluation of residual disease as a predictor of relapse in acute promyelocytic leukaemia. *The Lancet* 340(8833): 1437-1438

- Danhier F, Feron O, Pr  at V (2010). To exploit the tumor microenvironment: passive and active tumor targeting of nanocarriers for anti-cancer drug delivery. *Journal of controlled release* 148(2): 135-146
- De Jong WH, Borm PJ (2008). Drug delivery and nanoparticles: applications and hazards. *International journal of nanomedicine* 3(2): 133
- Denk W, Horstmann H (2004). Serial block-face scanning electron microscopy to reconstruct three-dimensional tissue nanostructure. *PLoS Biol* 2(11): e329
- Faraji AH, Wipf P (2009). Nanoparticles in cellular drug delivery. *Bioorganic & medicinal chemistry* 17(8): 2950-2962
- Foster KA, Yazdanian M, Audus KL (2001). Microparticulate uptake mechanisms of in-vitro cell culture models of the respiratory epithelium. *Journal of pharmacy and pharmacology* 53(1): 57-66
- Geissmann F, Manz MG, Jung S, Sieweke MH, Merad M, Ley K (2010). Development of monocytes, macrophages, and dendritic cells. *Science* 327(5966): 656-661
- Gnatenko DV, Dunn JJ, McCorkle SR, Weissmann D, Perrotta PL, Bahou WF (2003). Transcript profiling of human platelets using microarray and serial analysis of gene expression. *Blood* 101(6): 2285-2293
- Grayer RJ, Kite GC, Veitch NC, Eckert MR, Marin PD, Senanayake P, Paton AJ (2002). Leaf flavonoid glycosides as chemosystematic characters in *Ocimum*. *Biochemical systematics and ecology* 30(4): 327-342
- Haley B, Frenkel E. (2008). Nanoparticles for drug delivery in cancer treatment. Paper presented at the Urologic Oncology: Seminars and original investigations.

- Hayashi F, Means TK, Luster AD (2003). Toll-like receptors stimulate human neutrophil function. *Blood* 102(7): 2660-2669
- Huang X, Jain PK, El-Sayed IH, El-Sayed MA (2007). Gold nanoparticles: interesting optical properties and recent applications in cancer diagnostics and therapy.
- Hussain AI, Anwar F, Sherazi STH, Przybylski R (2008). Chemical composition, antioxidant and antimicrobial activities of basil (*Ocimum basilicum*) essential oils depends on seasonal variations. *Food Chemistry* 108(3): 986-995
- Jackson JK, Letchford K, Wasserman BZ, Ye L, Hamad WY, Burt HM (2011). The use of nanocrystalline cellulose for the binding and controlled release of drugs. *International journal of nanomedicine* 6: 321
- Janeway Jr CA., Medzhitov R (2002). Innate immune recognition. *Annual review of immunology* 20(1): 197-216.
- John R, Florence SS (2009). Structural and optical properties of ZnS nanoparticles synthesized by solid state reaction method. *Chalcogenide Lett* 6: 535-539
- Kolachana P, Subrahmanyam VV, Meyer KB, Zhang L, Smith MT (1993). Benzene and its phenolic metabolites produce oxidative DNA damage in HL60 cells in vitro and in the bone marrow in vivo. *Cancer research* 53(5): 1023-1026
- Lammers T, Kiessling F, Hennink WE, Storm G (2012). Drug targeting to tumors: principles, pitfalls and (pre-) clinical progress. *Journal of controlled release* 161(2): 175-187
- Liu T, Li L, Teng X, Huang X, Liu H, Chen D, Ren J, He J, Tang F (2011). Single and repeated dose toxicity of mesoporous hollow silica nanoparticles in intravenously exposed mice. *Biomaterials* 32(6): 1657-1668

- Lowenberg B, Downing JR, Burnett A (1999). Acute myeloid leukemia. *New England Journal of Medicine* 341(14): 1051-1062.
- Lu J, Liong M, Li Z, Zink JJ, Tamanoi F (2010). Biocompatibility, Biodistribution, and Drug-Delivery Efficiency of Mesoporous Silica Nanoparticles for Cancer Therapy in Animals. *Small* 6(16): 1794-1805
- Moghimi SM, Hunter AC, Murray JC (2001). Long-circulating and target-specific nanoparticles: theory to practice. *Pharmacological reviews* 53(2): 283-318
- Moghimi SM, Hunter AC, Murray JC (2005). Nanomedicine: current status and future prospects. *The FASEB Journal* 19(3): 311-330
- Moghimi SM, Szebeni J (2003). Stealth liposomes and long circulating nanoparticles: critical issues in pharmacokinetics, opsonization and protein-binding properties. *Progress in lipid research* 42(6): 463-478
- Mohanraj V, Chen Y (2007). Nanoparticles-a review. *Tropical Journal of Pharmaceutical Research* 5(1): 561-573
- Mondal A, Mishra S. (2014). Silica nanoparticles: synthesis and functionalization for drug delivery application.
- Moran AE, Carothers AM, Weyant MJ, Redston M, Bertagnolli MM (2005). Carnosol inhibits β -catenin tyrosine phosphorylation and prevents adenoma formation in the C57BL/6J/Min/+(Min/+) mouse. *Cancer research* 65(3): 1097-1104
- Morimoto K, Wolff S (1980). Increase of sister chromatid exchanges and perturbations of cell division kinetics in human lymphocytes by benzene metabolites. *Cancer research* 40(4): 1189-1193

- Muller J, Huaux F, Moreau N, Misson P, Heilier J-F, Delos M, Arras M, Fonseca A, Nagy JB, Lison D (2005). Respiratory toxicity of multi-wall carbon nanotubes. *Toxicology and applied pharmacology* 207(3): 221-231
- Mussai F, De Santo C, Abu-Dayyeh I, Booth S, Quek L, McEwen-Smith RM, Qureshi A, Dazzi F, Vyas P, Cerundolo V (2013). Acute myeloid leukemia creates an arginase-dependent immunosuppressive microenvironment. *Blood* 122(5): 749-758
- Nandiyanto ABD, Kim S-G, Iskandar F, Okuyama K (2009). Synthesis of spherical mesoporous silica nanoparticles with nanometer-size controllable pores and outer diameters. *Microporous and Mesoporous Materials* 120(3): 447-453
- Neuberger T, Schöpf B, Hofmann H, Hofmann M, Von Rechenberg B (2005). Superparamagnetic nanoparticles for biomedical applications: possibilities and limitations of a new drug delivery system. *Journal of Magnetism and Magnetic Materials* 293(1): 483-496
- Newman DJ, Cragg GM (2012). Natural products as sources of new drugs over the 30 years from 1981 to 2010. *Journal of natural products* 75(3): 311-335
- Ocaña A, Reglero G (2012). Effects of thyme extract oils (from *Thymus vulgaris*, *Thymus zygis*, and *Thymus hyemalis*) on cytokine production and gene expression of oxLDL-stimulated THP-1-Macrophages. *Journal of obesity* 2012
- Porcher C, Swat W, Rockwell K, Fujiwara Y, Alt FW, Orkin SH (1996). The T cell leukemia oncoprotein SCL/tal-1 is essential for development of all hematopoietic lineages. *cell* 86(1): 47-57
- Rowley JD (1980). Chromosome changes in acute leukaemia. *British journal of haematology* 44(3): 339-346

- Saha S, Mukhopadhyay M, Ghosh P, Nath D (2012). Effect of methanolic leaf extract of *Ocimum basilicum* L. on benzene-induced hematotoxicity in mice. *Evidence-Based Complementary and Alternative Medicine* 2012
- Sahu RK, Zelig U, Huleihel M, Brosh N, Talyshinsky M, Ben-Harosh M, Mordechai S, Kapelushnik J (2006). Continuous monitoring of WBC (biochemistry) in an adult leukemia patient using advanced FTIR-spectroscopy. *Leukemia research* 30(6): 687-693
- Sanvicens N, Marco MP (2008). Multifunctional nanoparticles—properties and prospects for their use in human medicine. *Trends in biotechnology* 26(8): 425-433
- Sarmiento B, Ferreira D, Veiga F, Ribeiro A (2006). Characterization of insulin-loaded alginate nanoparticles produced by ionotropic pre-gelation through DSC and FTIR studies. *Carbohydrate Polymers* 66(1): 1-7
- Schlenk RF, Döhner K, Krauter J, Fröhling S, Corbacioglu A, Bullinger L, Habdank M, Späth D, Morgan M, Benner A (2008). Mutations and treatment outcome in cytogenetically normal acute myeloid leukemia. *New England Journal of Medicine* 358(18): 1909-1918
- Sertel S, Eichhorn T, Plinkert PK, Efferth T (2011). Cytotoxicity of *Thymus vulgaris* essential oil towards human oral cavity squamous cell carcinoma. *Anticancer research* 31(1): 81-87
- Siegel R, Naishadham D, Jemal A (2013). *Cancer statistics, 2013*. CA: A Cancer Journal for Clinicians 63(1): 11-30
- Slowing II, Vivero-Escoto JL, Wu C-W, Lin VS-Y (2008). Mesoporous silica nanoparticles as controlled release drug delivery and gene transfection carriers. *Advanced drug delivery reviews* 60(11): 1278-1288

- Snyder R (2012). Leukemia and benzene. *International journal of environmental research and public health* 9(8): 2875-2893
- Soppimath KS, Aminabhavi TM, Kulkarni AR, Rudzinski WE (2001). Biodegradable polymeric nanoparticles as drug delivery devices. *Journal of controlled release* 70(1): 1-20
- Stone RM, O'Donnell MR, Sekeres MA (2004). Acute myeloid leukemia. *ASH Education Program Book* 2004(1): 98-117
- Su M, Alonso S, Jones JW, Yu J, Kane MA, Jones RJ, Ghiaur G (2015). All-trans retinoic acid activity in acute myeloid leukemia: role of cytochrome P450 enzyme expression by the microenvironment. *PloS one* 10(6): e0127790
- Terpinc P, Bezjak M, Abramovič H (2009). A kinetic model for evaluation of the antioxidant activity of several rosemary extracts. *Food Chemistry* 115(2): 740-744
- Von Ardenne M, Reitnauer P (1981). [The elevation of the leucocyte and thrombocyte counts produced by a thyme extract in the peripheral blood as compared to that caused by 2-cyanoethylurea (author's transl)]. *Die Pharmazie* 36(10): 703-705
- Wilczewska AZ, Niemirowicz K, Markiewicz KH, Car H (2012). Nanoparticles as drug delivery systems. *Pharmacological Reports* 64(5): 1020-1037
- Wisse E, Braet F, Luo D, De Zanger R, Jans D, Crabbe E, Vermoesen A (1996). Structure and function of sinusoidal lining cells in the liver. *Toxicologic pathology* 24(1): 100-111
- Yesil-Celiktas O, Sevimli C, Bedir E, Vardar-Sukan F (2010). Inhibitory effects of rosemary extracts, carnosic acid and rosmarinic acid on the growth of various human cancer cell lines. *Plant Foods for Human Nutrition* 65(2): 158-163

- Yunis JJ (1984). Recurrent chromosomal defects are found in most patients with acute nonlymphocytic leukemia. *Cancer genetics and cytogenetics* 11(2): 125-137
- Zhang Q, Wang X, Li PZ, Nguyen KT, Wang XJ, Luo Z, Zhang H, Tan NS, Zhao Y (2014). Biocompatible, Uniform, and Redispersible Mesoporous Silica Nanoparticles for Cancer-Targeted Drug Delivery In Vivo. *Advanced Functional Materials* 24(17): 2450-2461

thesis

ORIGINALITY REPORT

10%	4%	5%	6%
SIMILARITY INDEX	INTERNET SOURCES	PUBLICATIONS	STUDENT PAPERS

PRIMARY SOURCES

1	Submitted to Higher Education Commission Pakistan Student Paper	3%
2	doe.unimo.it Internet Source	1%
3	Tai, Joseph Cheung, Susan Wu, Matthew Ha. "Antiproliferation effect of rosemary (Rosmarinus officinalis) on human ovarian cancer cells in vitro", Phytomedicine: International Journal of , May 2012 Issue Publication	1%
4	TAIE, Hanan Anwar Aly. "Potential Activity of Basil Plants as a Source of Antioxidants and Anticancer Agents as Affected by Organic and Bio-organic Fertilization", Notulae Botanicae Horti Agrobotanici Cluj- Napoca/0255965X, 20100601 Publication	<1%
5	www.biomedcentral.com Internet Source	<1%
6	Cecilia Savii. "Recent Advances in Bioresponsive Nanomaterials", Carbon	<1%

-
- 7** Submitted to Doctor Harisingh Gour
Vishwavidyalaya, Sagar <1 %
Student Paper
-
- 8** arxiv.org <1 %
Internet Source
-
- 9** Cheung, Susan, and Joseph Tai. "Anti-proliferative and antioxidant properties of rosemary *Rosmarinus officinalis*", *Oncology Reports*, 2007. <1 %
Publication
-
- 10** www.science.gov <1 %
Internet Source
-
- 11** ccrcal.org <1 %
Internet Source
-
- 12** Juan L. Vivero-Escoto. "Mesoporous Silica Nanoparticles for Intracellular Controlled Drug Delivery", *Small*, 09/20/2010 <1 %
Publication
-
- 13** H. BUYUKHATIPOGLU. "A case representing coexistence of acute myeloblastic leukemia and dedifferentiated liposarcoma: the possible role of chemotherapy in triggering dedifferentiation", *Clinical and Laboratory Haematology*, 10/2006 <1 %
Publication
-